

# Laser Multiphoton Ionization-Dissociation Mass Spectrometry

D. A. GOBELI, J. J. YANG, and M. A. EL-SAYED\*

Department of Chemistry and Biochemistry, University of California, Los Angeles, California 90024

Received January 29, 1985 (Revised Manuscript Received June 19, 1985)

## Contents

I. Introduction	529	D. van der Waals Complexes	548
II. Theoretical Developments of Multiphoton Ionization and Dissociation	530	1. Metal Clusters	549
A. Contrasting Multiphoton Ionization-Dissociation Methods with Conventional Mass Spectrometry	530	2. Ammonia Clusters	550
B. Quasi-Equilibrium Theory (QET)	531	3. Benzene vdW Molecules	550
C. Statistical Approach to Fragmentation in MPIDMS	531	4. The Phenol Dimer and Toluene-Cyanobenzene Complex	550
1. Maximum Entropy Model	531	5. Fluorene vdW Molecules	550
2. Products Phase Space Model	531	6. Conclusion	551
3. Ladder Switching Model	532	VI. The Future of MPIDMS	551
4. Remarks on the MPID Statistical Approaches	532		
5. Comparisons Between the MPID Statistical Approaches and QET	533		
6. Discussion of the Theory of Conventional Mass Spectrometry	533		
7. Conclusions	534		
III. Historical Development of Multiphoton Ionization and Dissociation Techniques	534		
A. One-Photon Ionization	534		
B. Multiphoton Ionization	535		
C. MPID Mass Spectrometry	535		
1. Single Laser Experiments	535		
2. Multilaser Experiments	536		
3. Molecular Beam MPIDMS	536		
4. MPI Photoelectron Spectroscopy (MPIPES)	536		
IV. Studies of Diatomic Molecules	536		
A. Hydrogen (H <sub>2</sub> )	537		
B. Na <sub>2</sub> , Cs <sub>2</sub> , and PbTe and PbSe Vapors	537		
C. Iodine (I <sub>2</sub> )	537		
D. Nitric Oxide (NO)	538		
E. Carbon Monoxide (CO)	539		
F. Conclusion	539		
V. Studies of Polyatomic Molecules	539		
A. Small Polyatomics	539		
1. Nitrogen Dioxide and Nitrous Oxide	539		
2. Ammonia	540		
3. Methyl Iodide	540		
4. <i>trans</i> -1,3-Butadiene	541		
B. Medium-Sized Organic Molecules	541		
1. Benzene	541		
2. 2,4-Hexadiyne	543		
3. Benzaldehyde	543		
4. Acetaldehyde	545		
5. Aniline	545		
6. Tertiary Amines	545		
7. Alkylbenzenes and Halobenzenes	546		
8. Phenol	547		
C. Organometallics and Transition-Metal Complexes	547		

## I. Introduction

The use of high-intensity pulsed lasers has opened up new research areas. One of these is the study of the multiphoton absorption process. In these studies, a molecule absorbs more than one photon which can lead to dissociation (MPD) if the laser excites the vibrational motion in the ground electronic state. MPD is typically performed by using CO<sub>2</sub> or other infrared lasers. If the laser is capable of exciting electronic motion as well, ionization and dissociation can result (MPID). MPID is usually performed by using visible or ultraviolet (UV) lasers. It is the latter type of study that will be the subject of this review.

In some cases, multiphoton ionization dissociation (MPID) involves the simultaneous (coherent) absorption of more than one photon in the primary step to reach a resonant level. This is then followed by the sequential absorption of additional photons leading to ionization and/or dissociation. In most cases however, even the first absorption step involves a resonant (not a virtual) level. This leads to larger overall ion signals.

In the studies discussed here, the ionic fragments produced are detected by the use of mass spectrometry. Thus only ions are observed. Neutral species such as radicals are not examined. In some cases, they might actually be the main products of the interaction of the molecule with the high-intensity laser field. Due to the ease of ion detection however, our understanding of the mechanisms of the production of ionic fragments might progress faster than those for the production of neutral fragments by laser multiphoton absorption.

Since MPID mass spectrometry (MPIDMS), which is reviewed here, has a great deal in common with the field of mass spectrometry, we have attempted in this review to bring the two fields together so that a researcher in MPIDMS can be exposed to the methods and ideas present in the field of conventional mass spectrometry. Similarly, we hope to expose researchers in the field of mass spectrometry to the kinds of studies that have been going on in the field of MPIDMS during the past decade (1973-1984). We do not claim completeness of coverage in either field. For this we offer our apologies to those workers whose research was unintentionally not included.



David Gobeli was born in Lafayette, IN, in 1956. He received a B.S. (New Mexico) in 1976, a M.S. (Michigan State) in 1979, and a Ph.D. in 1984 for work in multiphoton ionization under Mostafa A. El-Sayed. He is currently an engineering specialist at Northrop Corporation in Hawthorne, CA.



J. J. Yang was born in Taiwan. She received a B.S. in Chemistry from National Taiwan University in 1978 and her Ph.D. in Chemistry in 1984 at the University of California, Los Angeles (with Professor M. A. El-Sayed). She was a guest scientist at the Max-Planck-Institut für Quantenoptik (Garching, West Germany) for part of 1982 during her graduate studies. She is now a postdoctoral member of the technical staff at AT&T Bell Laboratories. Her graduate major was in physical chemistry. Her doctoral research work was in the area of laser multiphoton ionization-dissociation mass spectrometry.



M. A. El-Sayed was born in Egypt in 1933. He obtained his B.Sc. degree from Ein Shams University, Cairo, Egypt in 1953 and his Ph.D. degree from Florida State University, Tallahassee, in 1959. He has held Research Associate (postdoctoral) positions at Harvard, Yale, and California Institute of Technology. He is currently on the faculty of the Department of Chemistry and Biochemistry at the University of California at Los Angeles, to which he was appointed in 1961. He was elected to the U.S. National Academy of Sciences in 1980 and has over 200 publications in the fields of electronic spectroscopy, molecular dynamics, laser time-resolved studies, photochemistry, and photobiology.

The outline of the review is as follows. We first contrast the theoretical ideas offered to explain ioni-

zation-fragmentation: (1) via an ionization source whose unit of energy is greater than the molecular ionization potential, such as 70-eV electrons, which are commonly used in conventional mass spectrometry, or 21.2-eV photons from a helium discharge, which are commonly used in conventional photoionization; (2) from a high-intensity UV or visible laser whose unit of energy is smaller than the molecular ionization potential. The theoretical section is then followed by a discussion of the experimental techniques in both mass spectrometry and MPIDMS. Examples of MPIDMS studies on diatomic molecules, polyatomic molecules, and clusters are then given in the last part of the review.

## II. Theoretical Developments of Multiphoton Ionization and Dissociation

### A. Contrasting Multiphoton Ionization-Dissociation Methods with Conventional Mass Spectrometry

Conventional ionization refers to electron impact (EI), charge exchange, and single-photon photoionization. The basic difference between conventional ionization methods and the MPI method is the mechanism of energy deposition into the reactant species. In conventional ionization or dissociation methods, an energy larger than the ionization potential is deposited in a single step which, coupled to the electron, leads to ionization first, followed by fragmentation. In the MPI method, the single photon energy is smaller than the ionization potential. This means that a multistep process is required in order to attain ionization or fragmentation. This leads to the following consequences. First, in MPI, the final species produced are a result of competition between further photon absorption and ionization, relaxation, or dissociation processes. The fragmentation pattern obtained depends upon the laser intensity, wavelength, and pulse width as these will determine the amount of energy deposited in the reactant species before its fragmentation. Second, at a fixed laser pulse width and excitation wavelength in MPI, the extent of fragmentation can be varied more easily (and more widely) than in conventional ionization methods simply by adjusting the laser intensity.

In general, the ionization-dissociation dynamics will depend upon the ionization method used. As an example, a molecule interacting with visible or UV laser radiation could dissociate prior to ionization (DI).<sup>1</sup> This is unlikely to occur using conventional ionization techniques. Ionization followed by dissociation (ID) is the most probable mechanism for the conventional ionization techniques, while both are possible in MPIDMS.

Besides the sequential photon absorptions that lead to the ID or DI mechanism in MPIDMS, fast pumping by a laser field with reasonable pulse width could lead to simultaneous absorption of several photons leading to a highly excited (superexcited) parent molecule. This highly excited parent molecule then "explodes" to give neutral or ionic (fragment) species. Combinations of the mechanisms in MPIDMS are also possible.<sup>1</sup>

In spite of these differences, a number of common problems exist in the statistical approaches for the interpretation of the resulting mass spectra for both types of ionization. This is because the statistical approach

depends not only upon the model itself but also on other factors such as the basic assumptions and the mathematical approximations for the density of states. Therefore, it is worth summarizing the original theoretical developments in the field of conventional mass spectrometry first, then discussing the different approaches in MPIDMS.

## B. Quasi-Equilibrium Theory (QET)

Quasi-equilibrium theory<sup>2-7</sup> was first proposed by Rosenstock et al.<sup>2,3</sup> and is the statistical theory originally derived for conventional mass spectrometry. In QET, it is assumed that the molecular processes leading to the formation of a mass spectrum consist of a series of competing, consecutive unimolecular decomposition reactions of vibrationally excited parent ions in their ground electronic state. Assuming the existence of equilibrium between reactants and activated complexes and the appropriateness of representing the system by a microcanonical ensemble, the rate constant for each of these reactions can be calculated from an absolute reaction-rate theory adapted to the experimental conditions of the mass spectrum (i.e., isolated system) by using a microcanonical ensemble. Thus, if an isolated system has an internal energy  $E$ , its rate of dissociation is given by

$$k(E) = \left( \frac{\alpha}{h} \right) \frac{W^\ddagger(E - E_0)}{\rho(E)} \quad (1)$$

where  $h$  is Planck's constant,  $W^\ddagger(E - E_0)$  is the number of vibrational and rotational states of the activated complex with an energy  $\leq (E - E_0)$ ,  $\rho(E)$  is the density of states of the reactant ion with energy between  $E$  and  $E + dE$ , and  $\alpha$  is the number of identical pathways for a particular reaction. As can be seen from the rate-constant expression, the calculation of  $k(E)$  lies mainly in the counting of states. Various mathematical approximations on the enumeration of states have been proposed. See ref 4-8 and references cited therein for details.

The calculation of a mass spectrum is done in the following manner. Kinetic rate equations are set up according to the proposed mechanisms and solved to obtain the ion yields in terms of rate constants and time. Then the rate constants as a function of excess internal energy are calculated, as well as the time scale of the mass spectrometer for a given accelerating voltage, geometry, and mass-to-charge ratio of the ion. The yield of each ion can be calculated as a function of the excess internal energy in the parent ion. The breakdown graph is then constructed. The actual mass spectrum is obtained by convolution of the breakdown graph with the internal energy distribution of the parent ion.

## C. Statistical Approach to Fragmentation in MPIDMS

There are three statistical models that have been derived for MPID so far: the maximum entropy model,<sup>9</sup> the products phase space model,<sup>10,11</sup> and the ladder switching model.<sup>12</sup> In these statistical models, the energy redistribution in the reactant ion is either tacitly or explicitly assumed to be complete before fragmen-

tation takes place. Fragmentation would therefore occur from the vibrationally excited ground-state electronic manifold of the reactant ions.

### 1. Maximum Entropy Model

The maximum entropy model of Silberstein and Levine<sup>9</sup> was the first statistical theory proposed to interpret the observed mass spectra by MPID. In this model, the most favorable fragmentation pattern is computed as the distribution in which the entropy of the system is maximized, subject to several constraints, including a given mean energy in each parent molecule and a given initial composition corresponding to a fixed number of independent parent molecules. The entropy is defined in terms of the counting of quantum states and thus takes into consideration the energetics and structure of the possible products. The fragmentation pathways for the formation of different fragments, however, are not imposed as part of the constraints and thus are not taken into account.

Several predictions that lead to computation-free tests of the theory can be made from the maximum entropy formalism.<sup>9,13</sup> First, for a given parent molecule, the fragmentation pattern is governed by the mean energy,  $\langle E \rangle$ , adsorbed per parent molecule. Thus, it should be possible to generate similar fragmentation patterns using the same excitation wavelengths as long as the internal energy deposited,  $\langle E \rangle$ , is the same (i.e., by adjusting the laser power) under each experimental condition. This gives the so-called "alternative ionization pathway test", which has been carried out by Lichtin et al.<sup>14</sup> on some polyatomic molecules. Second, the only way in which the parent molecule is specified in this formalism is in terms of its stoichiometric formula. Therefore, there is no distinction between isomers. Thus, it should be possible to generate similar fragmentation patterns if the mean internal excess energy deposited in each parent molecule is the same. One example performed in this direction is given in ref 15. Third, according to this formalism, the internal-state distribution of the fragments will be thermal in the statistical limit. Thus, the determination of the fragment's internal-state distribution provides the possibility of probing the statistical limit in detail. For examples of actual computational tests of the maximum entropy formalism, see ref 9, 13, and 16.

### 2. Products Phase Space Model

The second statistical model in MPID is the products phase space model that was proposed by Rebentrost and Ben-Shaul.<sup>10,11</sup> In this model, instead of maximizing the entropy of the system and neglecting the fragmentation pathways, the smaller ions are assumed to come from a tree of parallel (competitive) and consecutive fragmentation reactions of the parent ion. The excess energy required for fragmentation is assumed to be initially present in the parent ion. Based on the assumptions of loose transition states and a microcanonical products distribution, the probability of each fragmentation reaction can be calculated from the phase space occupied by the products as a function of distinct internal energies in the reactant and fragment ions ("infinite detection time" is inherently assumed here). At a given excess energy in the parent ion, one can calculate the probability of obtaining a particular ion

with different amounts of excess energy along a given reaction path. The internal energy distribution of each ion before fragmentation is obtained by summing the probability at each internal energy over all possible paths. The final probability of obtaining each ion (i.e., the relative abundance of each ion in the mass spectrum) can then be calculated by integrating the internal energy from zero to the minimal threshold for its further fragmentation. Thus, each ion yield can be obtained as a function of initial energy in the parent ion, and the breakdown graph can be constructed. The actual mass spectrum can be obtained by convolution of the breakdown graph with the internal energy distribution of the parent ion which, for instance, may be derived from the kinetic rate equation approach. This method has been used to calculate the mass pattern first for benzene<sup>10,11</sup> and recently for benzaldehyde and phenol.<sup>17,18</sup>

### 3. Ladder Switching Model

The ladder switching model, which is the third statistical model, does not treat excitation and fragmentation separately. It was proposed by Dietz et al.<sup>12</sup> and takes into consideration the competition between the unimolecular reaction and photon absorption during the light pulse. Thus, in a more exact sense, this approach is a combination of the kinetic rate equation and the statistical approaches. The basic idea of this treatment is as follows. The unimolecular reaction rates will become so fast with increasing excitation energy in the reactant ion that the competition for further photon absorption stops at a certain excitation energy, i.e., the energy point of competition (switching point). This "switching point" occurs where the rate of photon absorption is equal to the rate of the unimolecular dissociation reaction. After fragmentation occurs, the excitation ladder switches from the reactant to the product ion for further photon absorption ("ladder switching") if it is still within the laser pulse duration. In the simplified mathematical expression, the rate-equation approach is used (assuming that the nonradiative decay width of the electronically excited vibrational levels is greater than the Rabi frequency) to obtain the  $n$ -photon absorption probability as a function of laser intensity. The products phase space model is applied to calculate branching ratios and the energy distribution of products. Thus the energy distribution of each ion as a function of the  $n$ -photon absorption can be obtained. After the energy distribution is integrated from zero up to the switching point energy for each ion and is convoluted with the  $n$ -photon absorption probability, the final abundance of each ion can be obtained by summing the convoluted quantity over all possible  $n$ . The ion-yield curve for each ion can then be constructed as a function of laser intensity. The actual calculation was performed on benzene and compared with the experimental results of nanosecond pulsed lasers.<sup>12</sup>

### 4. Remarks on the MPID Statistical Approaches

Although some work has been done to test the validity of the current MPID statistical approaches with some molecular systems,<sup>9-13</sup> and they show at least qualitative agreement with experiment, the limited number of tests does not necessarily establish general

applicability of the statistical approaches to all molecular systems. Specifically, how the calculated mean energy deposited per parent molecule or parent ion can be related to the laser intensity employed during the experiment still remains an incompletely resolved problem. A kinetic rate equation approach, if valid, might be applied for such a purpose (for example, see ref 10-12). But information about the photon-absorption mechanism (i.e., simultaneous or sequential absorption in which resonant intermediate states are involved if it is a sequential absorption), the necessary photon-absorption cross section(s), and the spatial and temporal distributions of the laser pulse must be known before such detailed approaches can be performed. The use of a supersonic expansion will determine the initial state of the parent molecule and will simplify the theoretical derivation of the initial energy distribution in the parent species to some extent. In addition, the uncertainty of the input parameters involved in the calculations, such as thermodynamic data and spectroscopic information, might affect the results.

From a thermodynamic point of view, entropy and enthalpy factors determine the most favorable distribution (fragmentation pattern) of the system. The entropy factor tends to dominate as the temperature (i.e., the energy deposited into the system) increases. One would thus expect that the maximum entropy formalism is more applicable at the high-temperature (energy) limit. Since the energy is assumed to be initially deposited into the parent species, high laser intensity and reasonable pulse duration are required to obtain high-energy deposition before fragmentation. In this case, most of the photon absorption will occur via a parent-neutral ladder climbing process because the rate of photon absorption under high laser intensity is very likely to be faster than the rate of ionization of the parent molecule. A superexcited parent molecule is thus created and an "explosion" occurs.<sup>1</sup> The main factor in determining the fragmentation patterns produced via superexcited parent species is very likely the amount of energy deposited per parent species. This is because all reactions occur so fast and almost on the same time scale that it is no longer very significant to talk about mechanisms. Therefore, the maximum entropy formalism is expected to apply in the intensity region where parent-neutral ladder climbing takes place and a superexcited parent molecule is formed prior to any other reaction.

If the pumping rate of the parent ion is slower than the ionization rate but faster than the vibrational redistribution rate, multiply charged species and dissociation from unrelaxed repulsive surfaces are expected to dominate. If the rate of pumping in the parent ion is faster than the rate of ionization but slower than the relaxation rate, then the phase space or ladder switching mechanism is expected to describe the dissociation of the parent ion. If the rate of pumping in the parent molecule is slower than the rate of dissociation, then by treating the dissociated neutral as a new species with a given distribution of excess internal energy, the phase space or ladder switching model can also be used to describe the dissociation of the ion coming from the ionization of this new neutral species. The phase space and ladder switching models could be applied and extended to include the MPID patterns produced at



various excitation energies, with restrictions on the pulse duration and intensity when the pulse space model is used, since the energy is also assumed to be initially present in the parent ion.

In the statistical approaches, spectroscopic and thermodynamic information about the species considered is required. Uncertainties that might arise from these factors are inevitable. The maximum entropy model lacks in dynamical information but involves simple calculations. The phase space model is not always valid, but can give mechanistic information and involves simple computations. The lack of information available need not prevent the calculations from being carried out if educated guesses are made as to the important dissociation channels of the ions and the amounts of excess internal energies imparted to those ions.<sup>18</sup> The ladder switching model is the most applicable to the largest number of systems. However, as with the other models, it neglects switching of absorption to the neutral fragments and the introduction of ensembles with different angular momenta as a boundary condition. Photon-absorption properties as a function of excess internal energies of the ions at the specified laser wavelength are not generally known, which forces more assumptions to be made. The numerical computation is more complicated.

Due to unavoidable uncertainties that are involved in these statistical approaches for most applications, at the current stage, they should be used for interpretation, rather than prediction, of results.

##### 5. Comparisons Between the MPID Statistical Approaches and QET

The primary difference between the MPID and conventional ionization methods lies in the mechanisms of energy deposition into the reactant species. Since, under certain experimental conditions in MPID, excitation and fragmentation can be treated as separate processes, these ionization methods could become very similar in terms of excitation except that the initial energy distributions in the parent species might be different because of different Franck–Condon overlaps during excitation. Consider the mass spectrum produced from a parent species with a specific excess energy. The maximum entropy model and products phase space model do not possess general applicability to the MPID mass spectra, but the separation of excitation and fragmentation ladders in their formulation makes them somewhat similar to QET. The maximum entropy model may be more applicable in the high-temperature limit, which is more difficult to achieve by conventional ionization methods. In the products phase space model, excitation (in the parent ion) might also occur after ionization. This will not constitute the difference in the mass spectra produced by the products phase space model and QET if comparison is made starting from the same amount of excess energy in the parent ion (i.e., to eliminate the effect of different amounts of kinetic energies carried away by the ejected electrons during ionization by different methods).

Both the products phase space model and QET contain mechanistic information about the fragmentation process. The main difference is that QET uses a rate-constant expression equivalent to the unimolecular reaction expression derived from RRKM theory to cal-

culate the branching ratios. The products phase space model, however, uses a microcanonical model to calculate the branching ratios and energy distributions in the product ions. The QET used here for comparison is as it was originally derived. One might find a modified QET–phase space theory that can avoid the problem of defining an unknown transition state configuration.<sup>7</sup> This difference results in some advantages and some disadvantages in each case. First, the original QET formulation involves transition-state species rather than product species. The assumption of a “loose transition state” does not enter the original QET formulation. This assumption, which is involved in the products phase space model, can give energy distributions in the product ions, while in the original QET calculation, the energy is assumed to partition into the product species according to the number of internal degrees of freedom. However, there are fluctuations in the energy partitioning from this criterion.<sup>4</sup> Third, transition-state species are inaccessible to experimental measurement, and thus, the parameters of the transition-state species that are required for QET calculations are mostly unknown. The required parameters of the product species for the phase space model calculation, although still mostly unknown, are at least accessible to experimental measurement.

In conclusion, a theoretical (statistical) approach with general validity for MPID is much more complicated than for conventional mass spectrometry. This is due to the more complex excitation processes involved. Because of this complex excitation mechanism the MPI method is selective and versatile.

##### 6. Discussion of the Theory of Conventional Mass Spectrometry

Since QET was first proposed by Resenstock et al.,<sup>2,3</sup> extensive studies have been performed to test the validity of the theory. Due to certain difficulties encountered while testing the QET formalism, some of these studies lead to the modified theories such as that of Klots,<sup>19–25</sup> the adiabatic channel theory,<sup>26</sup> and the transition-state theory including nonadiabatic coupling effects.<sup>27</sup>

It is worth pointing out some information obtained from these investigations. First, the assumption of complete energy equilibration before dissociation might not strictly hold. An example of this would be the unexpected effects in organic mass spectrometry involving dissociation from isolated electronic states. These results are difficult to verify unambiguously however.<sup>7</sup> Second, the use of invalid mathematical approximations for the enumeration of the density of states may lead to noticeable disagreements between theory and experiment.<sup>4</sup> Various mathematical approximations have been derived and tested (see, for example, ref 4–8 and references cited therein). Third, although the statistical calculations demand knowledge of a variety of parameters that usually are not well-known and some fitting to the experimental data is nearly always required, some guidelines (i.e., for the choice of vibrational frequencies) can be followed. Moreover, it is demonstrated that the exact choice of the parameters is less critical than what might have been expected.<sup>7</sup> Fourth, some fragmentation reactions might have “tighter” transition states than others.<sup>7</sup>

Fifth, quantum corrections such as quantum mechanical tunneling and nonunity transmission coefficients in the rate-constant expression might be needed.<sup>4,6,8</sup> Sixth, the model of the one-dimensional dissociation coordinate accompanied by a set of oscillators whose function is to increase the energy-level density without any direct role in the reaction is a poor representation of a unimolecular dissociation. The unimolecular dissociation dynamics is an inherently multidimensional process, even for small polyatomic species.<sup>27</sup>

From the above discussion, it can be seen that useful information can be extracted from the previous developments in the field of conventional mass spectrometry for future detailed description of MPIDMS.

## 7. Conclusions

The general difficulties in the theoretical approaches are the existence of unknown molecular parameters necessary for calculations and, sometimes, their complexities. However, valuable information can still be obtained from the calculations by proper choice of the unknown parameters. Complicated calculations can be greatly aided by computer facilities. Due to the required conditions or assumptions involved in deriving the theoretical approaches, one should be careful about their applicable ranges.

The most complete model for MPID that has been derived thus far seems to be the ladder switching model. However, it still neglects the ladder switching of absorption to the neutral fragments, and it does not introduce ensembles with different angular momenta as a boundary condition. Also, if Rabi cycling is appreciable, the rate-equation formalism should be replaced by the density-matrix formalism.<sup>28</sup> Of course, this will make the entire derivation more complicated and its practical application more difficult, thus reducing its usability.

The great value of replacing conventional ionization methods by MPI in the mass spectrometer lies in the high selectivity of the MPI technique and thus its analytical potential. Therefore, it is certain that one of the goals of the statistical approaches is to accurately predict the mass spectra. However, it is equally important that these statistical approaches provide theoretical understandings of the fragmentation processes. To achieve these goals, the statistical nature of MPID needs to be tested more rigorously.

The MPI method generally has a more complicated mechanism in pumping energy into the reactant species than do the conventional ionization methods. In spite of this, it is expected that some of the problems encountered in performing the statistical calculations for MPIDMS might have already been answered from past studies in conventional mass spectrometry. Thus it is recommended that these not be treated as two completely separate branches of mass spectrometry.

### III. Historical Development of Multiphoton Ionization and Dissociation Techniques

Photoionization, whether induced by a laser or generated from a conventional light source, represents only a small fraction of the mass spectrometric research being performed at this time. Electron impact, by far, is the most prevalent ionization technique used. Other common ionization techniques include field ionization

and field desorption,<sup>29</sup> fast atom bombardment,<sup>30</sup> and desorption chemical ionization.<sup>29</sup>

The use of laser-induced multiphoton ionization in conjunction with mass analysis dates back only to about 1970.<sup>31,32</sup> Since it uses photons as an energy source, it could be considered as a subcategory of photoionization mass spectrometry, although it has very little in common with it either technically or theoretically. The next section of this review will trace the development of photoionization in mass spectrometry from its inception to the present-day usage of high-power pulsed lasers.

## A. One-Photon Ionization

The use of photons as an ionization source dates back to the infancy of mass spectrometry. Its first reported use came in 1929 by Ditchburn and Arnot<sup>33</sup> when potassium vapor was irradiated with the emission of an iron arc passing through the quartz windows of a magnetic-sector mass spectrometer. A more refined experiment was carried out in 1932 by Terenen and Popov<sup>34</sup> who used the isolated resonance lines of cadmium, zinc, and aluminum in conjunction with a simple magnetic mass analyzer to study the formation of ion pairs from thalium halides.

Before the true potential of this ionization technique could be realized, technical advances in vacuum technology and light sources as well as optical materials had to come. The next reported use of photoionization did not come until 1956 when Lossing and Tanaka<sup>35</sup> reported the photoionization mass spectrum of butadiene by the resonance lines of a krypton arc.

After the development of the vacuum ultraviolet monochromator for photoionization mass spectrometric studies by Hurzeler,<sup>36,37</sup> the constraints that were induced by having to find windows capable of transmitting the ionizing radiation were eliminated.

Several common light sources are generally used in the photoionization mass spectrometer. Rare gases in an electric discharge produce continua whose wavelength range depends upon the gas.<sup>35</sup> Hydrogen produces a many-lined spectrum which may also be used as a photoionization source.<sup>38</sup>

The major advantage of the use of photons to ionize species inside the mass spectrometer is their monochromaticity. This makes photoionization mass spectrometry a valuable tool in determining the ionization and appearance potentials.

The major drawbacks to using photons as an ionization source have been the experimental complexities and low signal levels involved with the use of vacuum ultraviolet radiation of wavelengths less than about 100 nm. This necessitates large pumping systems, several vacuum chambers, and a vacuum ultraviolet monochromator.

Because of the complexity and cost associated with a photoionization mass spectrometer, the device never really caught on (when compared with the electron impact mass spectrometer) as a common laboratory tool for routine analysis or identification. It does however have its place as an experimental tool in chemical physics for testing the theory of mass spectra due to the controlled manner in which energy can be deposited within the system.

The photoelectron spectrometer, which may have a laser multiphoton ionization source, may be placed in

a similar category. That is, because of the cost of such a device, it is rarely seen as a tool for routine laboratory analysis. A wealth of spectroscopic and dynamic information may be obtained from laser photoelectron spectroscopy. Therefore, this device is also of value to the experimental physical chemist.

## B. Multiphoton Ionization

Radiation from a pulsed laser can be of sufficient intensity to make multiple-photon processes (ionization for example) with visible laser light likely. This has eliminated the need for expensive vacuum equipment required in one-photon photoionization. In some instances, several photons may be simultaneously absorbed in a coherently driven process leading to ionization and fragmentation. If, however, there are electronic states resonant with the incident laser radiation, whether they be accessible by one- or two-photon selection rules, then resonance enhancement occurs and the resulting ion signal (if the resonant state is not dissociative) greatly increases. This is because the resonant intermediate state has a lifetime, sometimes on the order of the laser pulse duration, that permits sequential absorption of photons. Therefore, the required number of photons does not have to be simultaneously absorbed in order to reach the ionization or dissociation continuum as in the case with studies involving large polyatomic molecules.

MPI studies that would be of general interest to chemists did not start until well after the development of the dye laser several years later. Until that time, only a limited number of fixed-frequency laser wavelengths were available. Publications concerning the use of MPI as a spectroscopic device for studying two-photon states of molecules appeared in the mid-1970s by Johnson on the MPI spectra of NO<sup>39</sup> and benzene<sup>40</sup> and by Petty and Dalby<sup>41</sup> on the MPI spectrum of I<sub>2</sub>. A great amount of research on two-photon resonance, multiphoton ionization followed, in which two-photon states in the vacuum UV were studied with dye lasers in the visible region of the spectrum. MPI has been applied to the study of Rydberg states. Previous reviews of the MPI field are given in ref 42-44.

## C. MPID Mass Spectrometry

The use of the high-power pulsed laser as an ionization source in mass spectrometry preceded static-cell MPI work by several years. As early as 1970, pulsed lasers had been used successfully as ionization sources within the mass spectrometer.<sup>31,32</sup> In 1970, Bereshetskaya et al.<sup>31</sup> reported multiphoton ionization and fragmentation of H<sub>2</sub> using the output of a Nd:glass laser that produced 1.06- $\mu$ m photons. Although a low-resolution time-of-flight instrument was used in their investigation, the resolving capacity was sufficient to separate H<sub>2</sub><sup>+</sup> from H<sup>+</sup>. At about the same time, Chin reported on the use of laser radiation from a pulsed ruby laser system to study the multiphoton ionization of I<sub>2</sub>, CCl<sub>4</sub>, and D<sub>2</sub>O with a time-of-flight mass spectrometer.<sup>32</sup>

Further early work on the laser ionization mass spectrometric technique was performed by Letokhov et al.,<sup>45</sup> Schlag et al.,<sup>46</sup> Bernstein et al.,<sup>47</sup> Robin et al.,<sup>48</sup> and Zare et al.<sup>49</sup> At this point it had become clear that

MPI spectroscopy and conventional mass spectrometry were no longer mutually exclusive fields, and the potential of using MPIDMS in analytical chemistry had become obvious.

In its simplest form, a multiphoton ionization mass spectrometer consists of nothing more than a mass spectrometer with optical ports to permit the entrance of laser light. It is through the interaction of the laser light with the sample molecules that ions are formed.

Among the accessories currently being reported in the literature are molecular beams used in place of the conventional sample inlet systems<sup>50</sup> and electron kinetic energy analyzers used to complement the ion detection system.<sup>51</sup>

MPID mass spectra have been recorded on magnetic singly focusing instruments,<sup>52,53</sup> quadrupole mass spectrometers,<sup>54,55</sup> and time-of-flight mass spectrometers.<sup>56,57</sup> The time-of-flight mass spectrometer is usually the instrument of choice on which to perform mass spectrometric studies because an entire mass spectrum may be recorded for each shot of the pulsed laser. This makes data collection more efficient and may be an important factor considering the low repetition rates at which many pulsed lasers operate and the large number of spectra that might have to be averaged in order to produce a suitable signal-to-noise level.

The light source is almost always a high-power pulsed laser. It is the high peak powers that the pulsed laser is able to generate that allow multiphoton ionization/dissociation to occur. Other properties of laser radiation that are important to this form of mass spectrometry are its extreme monochromaticity and short pulse length.

### 1. Single Laser Experiments

With the several fixed-frequency pulsed lasers, dye lasers, Raman shifters, and other wavelength extenders that are now available, it is possible to generate laser radiation at suitable intensity to allow ionization at almost every frequency from about 200 nm into the infrared.

The most common lasers used in MPIDMS generate pulses on the nanosecond time scale. Although laser producing picosecond pulses have been around for some time, those capable of generating the peak intensities (several  $\mu$ J/pulse) necessary for ionization have only recently become commercially available. Therefore, they are not as common in MPIDMS yet as the nanosecond pulsed laser, which has been commercially available for some time. The power densities available from the focused output of most nanosecond pulsed lasers is on the order of GW/cm<sup>2</sup>, which is sufficient to ionize and dissociate most molecules that usually require 2-4 UV photons in order to reach the ionization continuum. Several reports have appeared in which picosecond lasers have been used to generate ions within the mass spectrometer.<sup>57-59</sup>

In a single laser experiment, the only variables are laser wavelength, intensity, and pulse width. In varying the laser intensity at a fixed wavelength, it is possible to perform a power dependence of the mass spectrum of the species being studied. The information that may be derived from such a study is of limited use however, since the changes in the mass spectra are usually complicated and not easily described.

By varying the wavelength of the laser, it is possible to generate the wavelength dependence of the mass spectra being recorded. This is also of limited use, because in many cases, the spectral features being observed in the mass-resolved ion current as a function of laser wavelength are all very similar to the static-cell MPI spectrum (in which the total ion current is collected).<sup>54</sup> This may be explained in terms of the spectral features arising from the rate-limiting step leading to the production of the individual fragment ions, which is usually the first absorption step from within the neutral manifold of the parent molecule.

## 2. Multilaser Experiments

By using more than one laser pulse, the potential information that can be derived from MPIDMS grows dramatically. In addition to having the added degrees of freedom of another laser pulse (power, wavelength, and pulse width), one can also vary the temporal delay between the two pulses. The potential power of such a combination has only begun to be explored.<sup>60-62</sup>

Such experiments include, but are not limited to, the determinations of excited-state lifetimes of the neutral molecules by varying the delay time between the two fixed-frequency laser pulses,<sup>63</sup> studies involving the ionization and fragmentation mechanism of a wide variety of molecular systems,<sup>60,61</sup> and studies involving the potential selectivity of the two-color technique in ionizing one component of a mixture whose ionization potentials are relatively close to one another.<sup>62</sup> Examples of multicolor MPIDMS experiments on specific molecules will be discussed later.

## 3. Molecular Beam MPIDMS

The motivation behind the introduction of a molecular beam system into the multiphoton ionization mass spectrometer is to take advantage of the large potential state selectivity that the nearly monochromatic radiation from a laser can offer and the mass spectrometric study of species that could only exist within the beam. Smalley et al.<sup>64</sup> did work in the application of molecular beams used as a source of state-selected molecules to the techniques of laser-induced fluorescence<sup>65,66</sup> and MPID.<sup>67,68</sup>

Although the study of the molecular beam is a complete field in its own right, it is generally treated as only a source of cold, state-selected molecules and exotic species such as van der Waals complexes in MPIDMS. For a complete review of the theory and applications of molecular beams, the reader is referred to the works of Smalley,<sup>64</sup> Anderson and Fenn,<sup>69</sup> and Kantrowitz and Grey<sup>70</sup> and references cited therein.

The molecular-beam output of a nozzle, which is either pulsed or continuous, is made to intersect the laser pulse at right angles along its center line axis. Ions created within the beam are accelerated into the entrance of the mass analyzer through the application of a voltage gradient. Sometimes it is desirable to use a skimmer<sup>67</sup> in conjunction with the nozzle. This may or may not require the use of a differential pumping arrangement and will result in a more collimated, well-defined beam.

Two types of beams exist: effusive and supersonic. When the ratio of the mean free path of the carrier gas to the nozzle diameter is very much less than 1, hy-

drodynamic conditions exist within the nozzle and cooling of the internal and translational degrees of freedom occurs. If the ratio is much greater than 1, effusive conditions exist within the beam, and the thermal properties of the expanded gas do not differ appreciably from those of the bulk.

The nozzle beam may either be pulsed or continuous. Pulsed sources offer the distinct advantages of producing instantaneously higher beam densities and requiring less expensive pumping systems. They are very suitable for use with pulsed lasers. Commercial valves with pulse durations of about 100  $\mu$ s are available.<sup>71-73</sup> In addition, plans for construction of homemade versions exist in the literature.<sup>74,75</sup> One of these uses an automobile pulsed fuel injector.<sup>75</sup> Continuous valves offer the advantage of being more reliable because there are no moving parts. Because of this however, the pumping requirements are more severe.

## 4. MPI Photoelectron Spectroscopy (MPIPES)

An MPI photoelectron spectrum is generated by collecting the electrons ejected in the multiphoton ionization process and then analyzing their kinetic energies. An MPI photoelectron spectrometer consists of an ionization source and associated ion optics, some form of electron kinetic energy analyzer, and a detector. Several types of electron kinetic energy analyzers are currently being used in MPI work, although numerous others have been used in conventional one-photon photoelectron techniques.<sup>76</sup>

MPI photoelectron spectroscopy has been performed on molecules to help elucidate the mechanism of multiphoton ionization.<sup>77-83</sup> It has also been used to study the ionization behavior of atoms.<sup>82,84-90</sup> As the resolutions of the MPI photoelectron spectrometer has been improved it has been used to determine the spectrum of the parent ions.<sup>82,87-94</sup>

When used in conjunction with a pulsed laser, the time-of-flight electron kinetic energy analyzer can record the entire spectrum for each laser pulse. This is important when considering the low laser fluxes that one is frequently forced to use in order to avoid loss in resolution due to space-charge effects.<sup>91</sup> Resolution of the time-of-flight instruments (about 3 meV) has recently advanced to the point to make photoelectron spectroscopy (vs. MPI mechanistic studies) practical.<sup>91,92</sup>

Arrival time of the photoelectrons is generally faster than for ions in a time-of-flight mass spectrometer. Factors that were not important in determining the resolution of the time-of-flight mass spectrum, such as influence from stray magnetic fields, must be considered when constructing a photoelectron spectrometer. Resolutions of time-of-flight electron kinetic energy analyzers generally range from 10 to 200 meV, limited by space-charge effects.<sup>92,95</sup>

Even though the time-of-flight electron kinetic energy analyzer appears to be gaining popularity, results have been published involving the electrostatic spherical sector analyzer.<sup>82,83,86</sup>

## IV. Studies of Diatomic Molecules

Diatomic molecules are the simplest category of molecules. The systems that will be discussed in this section are (A) H<sub>2</sub>, (B) Na<sub>2</sub>, Cs<sub>2</sub>, and PbTe and PbSe vapors, (C) I<sub>2</sub>, (D) NO, and (E) CO.



## A. Hydrogen (H<sub>2</sub>)

H<sub>2</sub> is the simplest molecule. Its photoionization dynamics are theoretically tractable; its excited states are well-characterized; and the rotational constant of its ion is extremely large.<sup>93</sup> This gives an advantage in choosing H<sub>2</sub> as a system for resonant MPI and photoelectron studies. The last feature makes the photoelectron spectra exhibit partially resolved rotational structure. This provides information on the partial waves of the ejected electron.

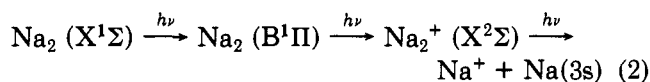
Early MPID studies of H<sub>2</sub> involved the use of excitation wavelengths at 1.06 μm<sup>91,92,96</sup> and 0.53 μm.<sup>97</sup> From the investigation of H<sup>+</sup> and H<sub>2</sub><sup>+</sup> signals as functions of laser intensity, various processes have been suggested to explain the observed behavior (i.e., power dependence) of H<sup>+</sup> and H<sub>2</sub><sup>+</sup> ions. However, as was pointed out by Lau,<sup>98</sup> H<sup>+</sup> ions observed in the MPI spectrum of H<sub>2</sub> by 0.53-μm radiation could also be formed by the ionization of H atoms in the *n* = 2 state, which were produced from photocatalytic processes.

A detailed resonant MPI study of H<sub>2</sub> involved the preparation of a resonant state by three-photon excitation of H<sub>2</sub>, X<sup>1</sup>Σ<sub>g</sub><sup>+</sup>, *v* = 0, *J* = 3, and subsequent ionization by a single additional photon.<sup>93</sup> The MPI spectrum of the complete B<sup>1</sup>Σ<sub>u</sub><sup>+</sup>, *v*' = 6 ← X<sup>1</sup>Σ<sub>g</sub><sup>+</sup>, *v*'' = 0 band and part of the *v*' = 7 band has been recorded. The results show that the P and R branches dominate the spectrum. There is little evidence for the N and T branches, which is in agreement with general predictions. In addition to the MPI spectrum, photoelectron spectra have also been obtained by pumping the P(3) and R(3) transitions of the B<sup>1</sup>Σ<sub>u</sub><sup>+</sup>, *v*' = 7 ← X<sup>1</sup>Σ<sub>g</sub><sup>+</sup>, *v*'' = 0 band.<sup>93</sup> Only the *v* = 0–3 levels of the H<sub>2</sub><sup>+</sup> X<sup>2</sup>Σ<sub>g</sub><sup>+</sup> state are energetically accessible with four photons under their experimental conditions. One interesting observation from this study was that the rotational structure changes qualitatively with the intermediate rotational level of the B<sup>1</sup>Σ<sub>u</sub><sup>+</sup> state. This directly reflects the selection rules for the ionizing transition.<sup>93</sup>

## B. Na<sub>2</sub>, Cs<sub>2</sub>, and PbTe and PbSe Vapors

Because previously reported experiments on the MPI of alkali atoms are often hindered by the presence of molecules in the vapor or atomic beam,<sup>99</sup> it has been suggested that the laser photodecomposition technique be used to reduce the molecular density in the atomic beam. The efficiency of the molecular laser photodecomposition technique depends on the wavelengths and intensity range of the laser used.

The resonant two-photon ionization of Na<sub>2</sub> and subsequent third-photon dissociation of Na<sub>2</sub><sup>+</sup> have been studied with the use of a pulsed dye laser.<sup>100</sup> The processes involved in the production of Na<sub>2</sub><sup>+</sup> and Na<sup>+</sup> ions are<sup>100</sup>



where the laser frequency is resonant with the B ← X vibronic transition (4926 Å for the B<sup>1</sup>Π (*v*' = 0) ← X<sup>1</sup>Σ (*v*'' = 0) transition). From the expressions for the time- and intensity-dependent populations of the ions and the fit to the observed ion signal variations with laser intensity, the photodissociation cross section of the X<sup>2</sup>Σ<sub>g</sub><sup>+</sup> state of Na<sub>2</sub><sup>+</sup> can be obtained.<sup>100</sup> From the measured

splitting of the Na<sup>+</sup> signal (due to separate detection of ions ejected toward and away from the detector) in the time-of-flight spectrum of the magnitude of the electric field, the kinetic energy given to the Na<sup>+</sup> ion during the dissociation process can be determined. This in turn gives the photodissociation energy of the Na<sub>2</sub><sup>+</sup> X<sup>2</sup>Σ<sub>g</sub><sup>+</sup> state.

The most efficient laser photodecomposition wavelength for the cesium dimer is at 758 nm.<sup>99</sup> This does not exactly coincide with the wavelength of maximum absorption of the B<sup>1</sup>Π ← X<sup>1</sup>Σ<sub>g</sub><sup>+</sup> band, which is at 760 nm at 550 K. This suggests the possibility of a second quasi-resonant step in the ionization process. The ionization potential of Cs<sub>2</sub> lies between 3.592 and 3.821 eV, requiring three 758-nm photons for ionization.<sup>99</sup>

It is found that at 758 nm,<sup>99</sup> photodissociation of the neutral dimers dominates the process for low laser intensity whereas three-photon ionization of dimers prevails for laser intensities higher than about 0.4 MW/cm<sup>2</sup>. The dissociation of neutral dimers is proposed to occur after a two-photon absorption.

The MPI studies of molecular cesium in the 6200–6500-Å region show that the dominant process for ionization is the two-photon photoionization through the intermediate C state of the cesium molecule.<sup>101</sup>

PbTe and PbSe vapors have been ionized via the resonant MPI process in a mass spectrometer.<sup>102</sup> It is found that the same spectral features are often observed in the photoionization cross section of the molecule and its component atoms. For instance, the spectra of PbTe<sup>+</sup> and Pb<sup>+</sup> between 23 000 and 24 000 cm<sup>-1</sup> are very similar, as are the spectra for Te<sub>2</sub><sup>+</sup> and Te<sup>+</sup> between 25 700 and 26 300 cm<sup>-1</sup>.<sup>102</sup> Thus, fragmentation after resonant excitation must be expected. In the PbSe vapor components, highly excited Pb atoms formed by the photodissociation of PbSe are resonantly excited to previously unreported, autoionizing, even-parity Rydberg levels by one-photon transitions. This Rydberg series converges to the 6p P<sup>0</sup><sub>3/2</sub> limit of Pb(II) at 73 900 cm<sup>-1</sup>. The three-photon ionization cross section containing two-photon resonant excitation is calculated for PbTe. The calculation shows that inclusion of intermediate vibrational sublevels in the resonant step results in the suppression of certain Franck–Condon peaks.

## C. Iodine (I<sub>2</sub>)

Molecular iodine, I<sub>2</sub>, has been extensively studied by optical spectroscopy due to its dense manifold of states.<sup>103</sup> Since it is a well-documented system and much is known about its spectroscopy,<sup>104</sup> this could be the reason that it has been chosen for many MPI studies in the past few years.<sup>41,47,54,103–107</sup> The first band system at 363–378 nm, a two-photon resonant, three-photon ionization series (Dalby's system), has a 0,0 band at 53 562 ± 4 cm<sup>-1</sup> and an excited-state vibrational frequency of 214 cm<sup>-1</sup>.<sup>47,54,103,105</sup> This band system is believed to be a low-lying Rydberg with a <sup>2</sup>Π<sub>1/2g</sub> I<sub>2</sub><sup>+</sup> core (i.e., 1g(<sup>2</sup>Π<sub>1/2g</sub>)nsσg).<sup>47,103,105</sup>

The second band system is found in the 402–415-nm (24 900–24 100 cm<sup>-1</sup>) region with a much lower ionization cross section than that of the Dalby system.<sup>103,107</sup> This system, with its 0,0 band at 48 426 ± 4 cm<sup>-1</sup> and a 254 ± 1 cm<sup>-1</sup> excited-state vibrational progression, is assigned to a two-photon resonant intermediate state in-

volved in either three- or four-photon ionization.<sup>103</sup> Polarization measurements and comparison to the Dalby system allow one to assign it as  $2g(2^2\Pi_{3/2g})ns\sigma g$ .<sup>103</sup> A number of atomic resonances are also observed in this region that are identified as resulting from the dissociation (predissociation) of iodine molecules followed by the ionization of excited iodine atoms.<sup>107</sup>

Other band systems are observed in the excitation into the visible  $B \leftarrow X$  in the MPI spectrum between 500 and 600 nm.<sup>47,54,103</sup> A dense set of multiphoton resonance ionization lines is observed. An intense system between 550 and 565 nm with a 0,0 band at  $35\,762 \pm 4\text{ cm}^{-1}$  and a  $104 \pm 1\text{ cm}^{-1}$  excited-state progression is assigned to a two-photon resonant intermediate state. The polarization measurement establishes it as  $O_g$ .<sup>103</sup>

The most striking feature about the resonant MPI spectra of  $I_2$  is the near absence of lines corresponding to the normal optical bands and also the absence of many possible multiphoton transitions allowed by selection rules. However, the cross section of the  $B \leftarrow X$  transition does occur prominently in the spectrum multiplicatively superimposed on the higher resonances.<sup>103</sup>

The mass-resolved analysis of the positive ions formed from the resonance-enhanced MPI of  $I_2$  shows that both  $I_2^+$  and  $I^+$  are produced.<sup>47,54</sup>

From the photoelectron and ion kinetic energy distributions of  $I^+$  and  $I_2^+$  ions following three-photon ionization of  $I_2$  resonantly enhanced via the two-photon allowed  $1 \leftarrow 0$  transition in the Dalby band, at 371.6 nm, the major fragmentation pathway for iodine is shown to follow additional absorption by the parent ion.<sup>106</sup>

Further MPI studies of  $I_2$  with two lasers (initiating laser at 596 nm and probing laser at 248 nm), detection of neutral fragments as well as positive and negative ions, and measurement of kinetic energies of fragments indicate the presence of two competing channels under these experimental conditions.<sup>104</sup> The low-energy channel proceeds through a two-photon intermediate state by the first laser. Absorption of one probe-laser photon leads to formation of the energetically lowest possible ion pair. The high-energy channel is consistent with a one-photon intermediate state and absorption of two probe-laser photons to form bound  $I_2^+$ . The molecular ion is subsequently photodissociated by an additional photon.

## D. Nitric Oxide (NO)

In the early stages of molecular MPI techniques, nitric oxide was chosen for study because of its stability and simplicity.<sup>108</sup> NO was the first molecule for which MPI was combined with supersonic cooling techniques.<sup>103</sup>

Most of the studies on NO by MPI<sup>39,42,45,54,56,77,82,88,108-117</sup> with resonant intermediate states can be classified into two categories. The first corresponds to the '3 + 1' (three-photon resonant, four-photon ionization) process.<sup>42,77,108,109</sup> The second corresponds to the '2 + 2' (two-photon resonant, four-photon ionization) process.<sup>42,82,88,108-111,116</sup>

The multiphoton ionization spectrum of nitric oxide cooled by a supersonic expansion has been recorded in the 400-490-nm region.<sup>108</sup> Rotational cooling has al-

lowed analysis of the two- and three-photon resonances in the four-photon ionization spectrum within this wavelength region, showing that the simple extension of one-photon intensity relationships to the three-photon spectrum does not adequately explain the features observed therein.<sup>108</sup> The expected strong np bands are not present in the MPI spectrum; the vibrational progression of the 3d complex appears in the MPI spectra with enhanced intensity relative to the one-photon absorption. The causes of intensity differences between the three-photon resonant MPI spectrum and the one-photon spectrum could be due to the differences in the photon absorption cross sections, competition between ionization, and other processes such as dissociation, predissociation (many states of NO have a high probability for predissociation), and fluorescence.<sup>39,108</sup>

A theoretical analysis of the multiphoton ionization spectrum of NO was carried out by both the perturbation (short-time) and rate-equation (long-time) descriptions of the stepwise excitation and ionization process.<sup>108,109</sup> Both approaches give qualitatively similar results.<sup>109</sup> The '2 + 2' and '3 + 1' processes in the four-photon absorption were addressed. The higher intensity of the '2 + 2' process,<sup>42,108,109</sup> which is in agreement with the kinetic treatment,<sup>42,108</sup> can be explained from the perturbation description to be due to large dipole matrix elements and an extra channel involved in the '2 + 2' process for the wavelength range considered. The kinetic approach is not required to explain the large difference between the '2 + 2' and '3 + 1' intensities. This is because the primary differences between these two processes are inherent in the absorption coefficients, and therefore taking the time dependence into account could only increase the ratio of the two intensities.<sup>109</sup> Despite the good agreement in the relative intensities of different transitions between experiment and the theoretical perturbation results,<sup>109</sup> some anomalies point to the necessity of including dissociation in the kinetic scheme as well as considering the ionization cross section for some excited states where the transition probability to the continuum is small.<sup>42</sup>

Efforts have also been directed to the photoelectron kinetic energy<sup>77,82,88,114</sup> and angular distribution<sup>77</sup> analyses of NO following its ionization. In the case of four-photon ionization resonant with various vibrational levels (ranging from 0 to 3) of the two-photon allowed  $A^2\Sigma^+$  state<sup>82,88</sup> and three-photon ionization resonant with the two-photon 0 and 1 vibrational levels of the  $C^2\Pi$  state,<sup>82</sup> the direct ionization pathway has been observed. In the former case, the presence of a near-zero energy electron peak suggests a second process that leads to ionization.<sup>82</sup> Further investigation of the four-photon ionization resonant with 0 and 1 vibrational levels of the two-photon  $A^2\Sigma^+$  state reveals the possibility of preionization via a dissociative channel.<sup>88</sup>

In the '3 + 1' process in NO, the photoelectron kinetic energy analysis reveals that ionization through the Rydberg F and H ( $H'$ ) states at the ground and first excited vibrational levels gives rise to the ground electronic state of the ion in the ground and first excited vibrational levels, respectively (i.e., a  $\Delta v = 0$  transition). Photoelectron angular distribution analysis reveals that the '3 + 1' process may be interpreted in terms of co-

sine-square distributions, strongly indicating that the ionization step takes place by one-photon direct ionization from the three-photon resonant states.<sup>77</sup>

### E. Carbon Monoxide (CO)

Unlike NO, most other diatomic molecules such as CO have relatively high ionization potentials, incompletely characterized spectra in the visible and UV, and relatively closely spaced electronic states in the ion.<sup>94</sup> Thus MPI dynamical studies by the analyses of photoelectron kinetic energy and angular distributions from MPI of such molecules become considerably more complex. However, CO has been chosen for study using MPI photoelectron techniques.

The MPI studies of CO by Pratt et al.<sup>94</sup> involves a three-photon resonance to the  $v = 1-3$  levels of the CO  $A^1\Pi$  state (laser wavelength from 434–454 nm) followed by the absorption of either two ( $v = 3$ ) or three ( $v = 1, 2$ ) additional photons to reach the ionization continuum. The first measurement is the wavelength dependence of the  $CO^+$  ion intensity,<sup>94</sup> which yields the rotational structure of the intermediate resonant state. The partially resolved rotational lines can be completely accounted for by the P, Q, and R branches observed in single-photon absorption studies. The N, O, S, and T branches are absent, which is in agreement with the three-photon fluorescence excitation spectra. The second measurement is the kinetic energy spectra of the ejected electrons resulting from ionization at wavelengths corresponding to the R-branch bandheads of the  $A^1\Pi v = 1-3$  levels.<sup>94</sup> Vibrational branching ratios in these photoelectron spectra do not follow the pattern predicted by the Franck-Condon overlap either between the intermediate  $A^1\Pi$  state and the ionization continuum or between any perturber of the  $A^1\Pi$  state and the ionization continuum. Accidental resonances at the four-, five-, and six-photon levels play a major role in determining the vibrational branching ratios. Other factors that may be responsible for the observed deviations from simple Franck-Condon distributions are (1) electronic and vibrational autoionization, (2) the possible strong energy dependence of the electronic part of the dipole element coupling the intermediate resonant state to the ionization continuum, thus modifying the photoelectron intensity as a function of kinetic energy, (3) the possible failure of the Franck-Condon separation itself due to the sharp variation of any component dipole matrix element with internuclear distance, and (4) the possible invalidity of an overall Franck-Condon factor for a multiphoton process in terms of the resonant intermediate states.<sup>94</sup>

MPI of CO at 248 nm<sup>117</sup> requires a minimum of three photons to reach the ionization energy of 14.0 eV. The power dependence is consistent with a three-photon process.

### F. Conclusion

From the above studies, it is clearly seen that the determination of photoelectron kinetic energy and angular distributions following MPI provides useful information about the dynamics of the MPI process. Similarly, the fragment ion kinetic energy analysis also gives insight to the MPI fragmentation mechanisms. Since a detailed analysis of these measurements will be partially based upon the well-characterized vibronic

spectra of the parent molecules (as can be viewed by comparing CO with NO), small polyatomic molecules, especially the diatomics, are potential candidates for such studies because of their simplicity, their amenability to theoretical analysis, their understood vibronic structures, and their readily interpreted photoelectron spectra. Thus, the kinetic energy and angular distribution analysis of photoelectron and fragment species (of small molecules such as diatomics) will be expected to represent one of the major research areas for the studies of MPID in the very near future.

## V. Studies of Polyatomic Molecules

The multiphoton ionization mass spectrometric study of polyatomic molecules is divided into four categories. These are (1) small polyatomics, (2) medium-size organics, (3) organometallics and transition-metal complexes, and (4) clusters and complexes. The ionization and fragmentation behavior displayed by each class of molecule differs in general.

### A. Small Polyatomics

In the following subsections, the following small polyatomics will be discussed: (a)  $NO_2$  and  $N_2O$ , (b)  $NH_3$  and  $ND_3$ , (c)  $CH_3I$ , and (d) *trans*-1,3-butadiene.

#### 1. Nitrogen Dioxide and Nitrous Oxide

Two-color photoionization experiments<sup>45,63,118,119</sup> have been performed on  $NO_2$  (IP = 9.78 eV). In these experiments, the exciting and ionizing laser pulses were synchronized. The exciting laser was scanned through the 440–470-nm region and the ionizing laser was fixed at 160 nm.<sup>45,63</sup> It was found that  $NO_2^+$  was the only observed species under these experimental conditions. The first laser was used to excite the system within the  ${}^2B_1 \leftarrow {}^2A_1$  absorption manifold. This was concluded to be the rate-limiting step in the ionization process as the  $NO_2$  current had a similar wavelength dependence to the  ${}^2B_1 \leftarrow {}^2A_1$  optical absorption spectrum.

Single-frequency MPI work has also been performed on  $NO_2$  in the visible,<sup>120,121</sup> UV (at 248 nm), and vacuum UV (at 193 nm)<sup>122</sup> regions. In a detailed study of the visible region of the spectrum,<sup>121</sup> MPI spectra were recorded from 520 to 420 nm at a pressure of 2 torr in a static cell and in a mass spectrometer under low-pressure conditions using both a conventional inlet and molecular beam systems. The results show that above 500 nm, under both collision-free and moderate-pressure conditions, the dominant pathway leading to ionization is a four-photon direct absorption process to yield predominantly  $NO_2^+$  with resonant enhancement occurring at the third photon level due to the  $3s\sigma$  Rydberg state. Below 500 nm, a rapidly increasing fraction of  $NO_2$  molecules dissociate at the two-photon level ( $B {}^2B_2$  state) to form  $NO + O$ . In this wavelength region the multiphoton ionization spectrum becomes increasingly characteristic of NO as less  $NO_2$  remains to be ionized.

Between 475 and 490 nm, the two-photon photodissociation of  $NO_2$  yields primarily  $NO (X^2\Pi) + O ({}^3P)$  with an excess energy of approximately  $15\,000\text{ cm}^{-1}$  deposited in the NO vibration. The MPI spectrum of NO in this region is congested with hot bands. Below about 475 nm, the  $NO (X^2\Pi) + O ({}^1D)$  channel domi-

nates the two-photon photodissociation at low pressures. This is reflected in the appearance of substantially less energy in the NO vibration. The static-cell MPI spectrum of NO<sub>2</sub> that was taken under higher pressures (2 torr) remains congested all the way down to 420 nm. The transition from one photodissociation channel to the other is abrupt at low pressure, occurring as soon as it is energetically possible.<sup>121</sup> The two-photon dissociation channels of NO<sub>2</sub> below 500 nm are thus wavelength and pressure dependent.

The single-frequency MPI of NO<sub>2</sub> at 248 and 193 nm<sup>122</sup> shows the formation of NO<sup>+</sup> comes mainly from the dissociation of NO<sub>2</sub><sup>+</sup> (i.e., ionization preceding dissociation). O<sub>2</sub><sup>+</sup> is also present, but only as a minor component of the total ion current. It was suggested that it arises from the dissociation of NO<sub>2</sub><sup>+</sup>.

N<sub>2</sub>O has also been the subject of MPI studies at 193 nm.<sup>122</sup> The principal product ion from N<sub>2</sub>O is NO<sup>+</sup> with minor amounts of N<sub>2</sub>O<sup>+</sup> and O<sup>+</sup> also present. The three-photon ionization of N<sub>2</sub>O may yield N<sub>2</sub>O<sup>+</sup> with sufficient excess internal energy to dissociate into NO<sup>+</sup> and N. The multiphoton formation of O<sup>+</sup> at 193 nm is attributed to the dissociation of N<sub>2</sub>O into N<sub>2</sub> and O (<sup>1</sup>D) followed by the two-photon ionization of O (<sup>1</sup>D).<sup>122</sup>

## 2. Ammonia

MPI has been used to extensively study the excited electronic states of NH<sub>3</sub>. New assignments of these excited electronic states have been made.<sup>123-126</sup> Expansion-cooled NH<sub>3</sub> has been studied in the 380–500-nm region with MPI and in the vacuum UV region at 125–160 nm.<sup>126</sup> Three of the five previously reported states have been reassigned. Seven additional states have been reported and assigned. These assignments are made possible because of the spectral simplification provided by the rotational cooling caused by the supersonic expansion as well as the difference in selection rules between multiphoton and one-photon processes.

Among the five previously reported states A, B, C, D, and E, the latter three are reassigned. Through these states, ionization occurs via four-photon processes except for B(*v*<sub>2</sub>1), B(*v*<sub>2</sub>2) and B(*v*<sub>2</sub>3), which result from five-photon ionizations. All of these ionization processes have three-photon resonances except for the A state, which represents two-photon resonant excitation. One principal conclusion resulting from this study is that nd orbitals must be included in any description of the NH<sub>3</sub> excited-state manifold. This is because of the intense features for which they are responsible in the vacuum UV spectrum,<sup>126</sup> which is in contrast to the previous experimental and theoretical work where they were excluded from consideration. There is also evidence for direct competition between photodissociation and photoionization in the NH<sub>3</sub> excited states.<sup>126</sup>

Comparable bands for ND<sub>3</sub> were also recorded and analyzed with the static-cell technique,<sup>123,124,126</sup> which helped in the investigation of the electronic states of NH<sub>3</sub>.

Mass spectrometric studies,<sup>51</sup> photoelectron energy studies,<sup>51,77</sup> and angular distribution analysis<sup>77</sup> following the resonantly enhanced four-photon ionization of NH<sub>3</sub> have been performed by using the A, B, C', and D states as resonant intermediates. The results demonstrate that the MPI mechanism of NH<sub>3</sub> involves climbing two different ladders.<sup>51</sup> First, the system climbs the ladder

of neutral states until the ionization potential is reached, followed by ionization or autoionization. Photoexcitation of the resultant ions to a state capable of dissociation then follows. Thus, ion production and ion dissociation are distinct processes. Three ionization mechanisms are proposed.<sup>51</sup> The first involves vibrational autoionization, as observed in the B state.<sup>51,77</sup> The second involves the production of vibrationally state-selected ions. This mechanism occurs only in the C' state.<sup>51,77</sup> The third mechanism involves rapid internal conversion in the neutral manifold followed by excitation to quasi-discrete states which then autoionize. This is observed in the A and D states.<sup>51</sup> These proposed ionization mechanisms are based upon photoelectron studies.<sup>51,77</sup> Low (~0 eV) kinetic energy electrons are produced following ionization of the A, B, and D resonantly excited intermediate states, the origin of which is thought to be due to vibrational autoionization. Higher photoelectron energies are obtained following ionization through the several measured C' vibronic intermediate states that correspond to direct ionization. The one-photon direct ionization from one of the three-photon resonant C' vibronic states is further confirmed by the cosine-square distribution of the photoelectron angular dependence.<sup>77</sup>

The mass spectral results of ammonia reveal an energy threshold for fragmentation,<sup>51</sup> which corresponds to the minimum number of photons required to reach the first excited state of the ion. There is no evidence that the nature of the intermediate bound state seriously affects the fragmentation pattern.<sup>51</sup> Due to the large separation of the electronic states in the ammonia ionic manifold (i.e., about 5 eV), the nonradiative rate is expected to be small. Therefore, it is unlikely that the electronic excitation of the NH<sub>3</sub><sup>+</sup> ion will be quenched rapidly by nonradiative transitions and that all of the energy pumped into NH<sub>3</sub><sup>+</sup> will appear as rovibrational energy in the ground electronic state, which leads to fragmentation.<sup>51</sup>

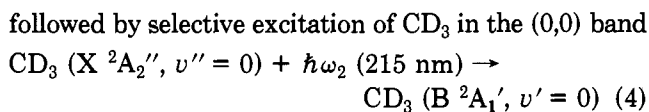
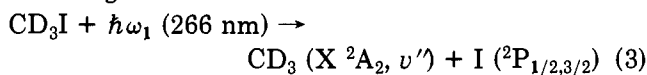
## 3. Methyl Iodide

The 6s ← 5pπ Rydberg states of methyl iodide and methyl iodide-*d*<sub>3</sub> have been investigated by two-photon resonant MPI in the 49 000–55 000-cm<sup>-1</sup> region.<sup>127</sup> In the 6s ← 5pπ excitation, four separate transitions to excited states labeled Δ, Π, Σ, and Π in increasing energy are expected.<sup>127</sup> The Σ<sup>+</sup> ← Σ<sup>+</sup> transition, although extremely weak in the one-photon absorption spectrum, has been identified by laser polarization studies and directly observed to be a strong feature in the MPI spectrum. Rotational contours indicate a large geometry change in this transition. The two Π states appear strongly in both the one- and the two-photon spectrum. No evidence is found of the Δ ← Σ<sup>+</sup> transition by MPI even though it is symmetry allowed. This could be due to a very small two-photon absorption cross section, a low probability of detection by ionization, or a combination of both.<sup>127</sup>

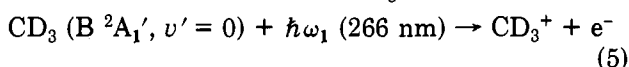
MPI studies of methyl iodide were also performed in the 7100–5300 and 3550–2650-Å regions to look into the nature of the σ\* ← n A-band system and its photochemistry.<sup>128</sup> The 6p ← 5pπ Rydberg excitations of methyl iodide-*h*<sub>3</sub> and -*d*<sub>3</sub> are observed as two-photon resonances when excited in the 28 000–32 000-cm<sup>-1</sup> region.<sup>128</sup> From considerations of vibrational frequencies

and intensities, the symmetries of the upper state components of this two-photon allowed transition have been assigned to  $A_2(3/2)$ , and its spin-orbit counterpart to  $A_2(1/2)$ . The two-photon methyl iodide resonances abruptly cease at  $32\,000\text{ cm}^{-1}$ . At higher frequencies they are replaced with those of iodine and methyl fragments. This correlates directly with the onset of a one-photon intermediate resonance in the A band of methyl iodide. In contrast, when pumping with light of one-half the above frequencies, i.e., beyond  $16\,000\text{ cm}^{-1}$ , to achieve a two-photon resonance in the A band, no fragment signals are observed. Instead, one sees three-photon resonances to the  $(5p\pi, 6s)$  states of the parent molecule. This leads one to believe that the A-state components reached with a single UV photon are dissociative, whereas the component ( $A_2$ ) reached with two visible photons of equivalent energy is bound for at least 10 ns.<sup>128</sup>

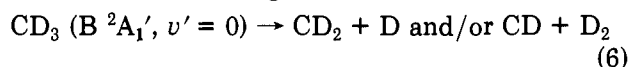
Two-color collisionless MPI experiments on methyl iodide- $h_3$  and - $d_3$  have been performed by using 266 nm ( $1 \times 10^{-7}\text{ W/cm}^2$ ) radiation and tunable radiation around 215 nm ( $2 \times 10^6\text{ W/cm}^2$ ).<sup>129</sup> The timing of the two laser pulses is such that they coincide within the ionization region, with jitter of about 1 ns. The 215-nm wavelength is chosen because the methyl radicals  $\text{CH}_3$  and  $\text{CD}_3$  absorb there resonantly through the  $(0,0)\text{ B }^2A_1' \leftarrow \text{X }^2A_2''$  transition with the B state being very heavily predissociated.<sup>129</sup> When the 266-nm and 215-nm (tuned to  $\text{B} \leftarrow \text{X}$ ) pulses are applied simultaneously, the  $\text{CD}_3^+$  is predominantly determined by the following mechanism:<sup>129</sup>



and ionization of the excited  $\text{CD}_3$



This ionization step competes with the fast predissociation into neutral fragments



The same mechanism applies to  $\text{CH}_3^+$ , for which the dissociation rate in the B state is 10 times faster and the ionization yield correspondingly smaller.<sup>129</sup>

$\text{CH}_3\text{I}$  is also one of the target molecules for which the statistical fragmentation patterns are calculated by the maximal entropy model<sup>13</sup> and on which the experimental appraisal of the maximal entropy theory is performed by the alternative ionization pathway test.<sup>14</sup>

#### 4. *trans*-1,3-Butadiene

*trans*-1,3-Butadiene is an example in which the multiphoton selection rules are effective in removing the restrictions on transitions of molecules with a center of inversion. It is the smallest polyene and a subject of extensive theoretical investigation.<sup>130,131</sup> The MPI spectrum of *trans*-1,3-butadiene has been measured in the 365–468-nm region,<sup>42,130</sup> which covers most of the region of interest for the bound states of the molecule. A two-photon allowed transition has been observed with

one-photon energy above 405 nm. From the vibronic structure of this state, it has been assigned as having  $^1B_g$  symmetry.<sup>130</sup> The polarization characteristics of the MPI spectra are consistent with the symmetry assignment of the two-photon state.<sup>28,132</sup> Investigation of the pressure broadening of the thermal lensing spectra confirms the Rydberg assignment for the g state.<sup>131</sup> Besides this two-photon allowed transition, many three-photon resonances with Rydberg states are observed in the four-photon ionization. This corresponds to laser photons with less energy than 405 nm. A new series with a quantum defect of 0.04 is identified.<sup>130</sup> However, within the energy region studied ( $42\,700$ – $54\,800\text{ cm}^{-1}$  in two-photon energy) no state was found for which the  $^1A_g$  symmetry designation could be made.<sup>130</sup>

The laser ionization mass spectrometric experiments have also been performed on *trans*-1,3-butadiene at an excitation wavelength of 368.8 nm,<sup>54,116</sup> which shows that the REMPI process yields considerably more fragmentation than does EI.<sup>45,54,116</sup> An analysis of the energetics of fragment ion formation has shown that at least six UV photons are absorbed per parent molecule undergoing REMPI at the 0,0 resonance near 387 nm.<sup>54,116</sup>

## B. Medium-Sized Organic Molecules

### 1. Benzene

Benzene has been the most extensively studied molecule to date using MPIDMS.<sup>46,55,57,59,133–143</sup> In addition to this, photoelectron<sup>81,106</sup> studies and some theoretical work<sup>10–12,14</sup> have also been done on this molecule.

The mechanism by which benzene ionizes and fragments was first studied in detail by Schlag and his group in a series of experiments over several years. In the earliest of these,<sup>46</sup> the doubled output of a  $\text{N}_2$ -pumped dye laser was used to ionize benzene by a one-photon resonant ( $6^1$  transition within the  $^1B_{2u}$  manifold), two-photon ionization process. It was shown that under “soft” ionization conditions, it was possible to create exclusively the molecular ion. It was also noted that a small peak which occurred at  $m/e$  79 corresponded to heavy benzene ( $^{12}\text{C}_5^{13}\text{CH}_6$ ). In a natural mixture of benzene, this species should represent approximately 6% of all species that are present. It should be noted that in the MPI mass spectrum the peak intensities will not necessarily be in this ratio owing to the different absorption cross section of the two species at the laser wavelength being used. This was the basis of the isotope separation experiments originally proposed by Letokhov.<sup>144</sup>

In the original experiments, one- and two-color techniques were used in conjunction with a quadrupole mass analyzer. It was reported by Boesl et al.<sup>59</sup> that under some circumstances it was desirable to use the quadrupole mass analyzer as a simple time-of-flight mass spectrometer. This could be done by applying no ac signal to the quadrupole rods and using the device simply as a drift tube. This had the advantage of generating an entire mass spectrum in a single laser pulse.

In the same publication,<sup>59</sup> the fragmentation mechanism of benzene was examined after it was shown that



the parent ion could be exclusively generated by exciting the  $6^{113}$  transition within the  $^1B_{2u}$  manifold with 241.61 nm radiation, by a one-photon resonant, two-photon ionization process. After 17 ns, a second laser pulse of wavelength 483.2 nm was brought into common focus with the first pulse. This caused extensive fragmentation of the parent ion.

The total integrated ion current did not change however. This indicated that the new ions may be created from the molecular ion. Because of the delay, excitation of  $^1B_{2u}$  benzene by the visible laser pulse was precluded. These results indicate that the parent ion may be the predecessor of all other fragment ions in the benzene MPID. The neutral absorbing past the ionization threshold to a superexcited state can be ruled out under these experimental conditions.<sup>14</sup>

In a similar experiment,<sup>135</sup> it was shown that under conditions of moderate laser power, ionic fragments created by the absorption of photons by the parent ion can also absorb photons to create even smaller fragments. This was done by separating the different fragments in the acceleration region of a time-of-flight mass analyzer and then selectively exciting certain packets of ions. It therefore becomes possible to selectively irradiate specific ion packets ( $C_4H_X^+$  for example where  $X = 0, 1, 2, 3, 4$ ) created by the first pulse by the second pulse and measure the subsequent change in the fragmentation pattern on the basis of the distance from the ionization source.

In another early experiment, Zandee et al.<sup>54</sup> examined the fragmentation of benzene utilizing a single-color quadrupole technique. The laser wavelength was first chosen to be variable, ranging between about 385 and 395 nm. This represents a two-photon absorption within the  $^1E_{1g}$  manifold. The mass-resolved ion current was taken as a function of wavelength for each group of fragments ( $C_1$ -containing species,  $C_2$ -containing species, etc.). The resulting production spectra were found to be quite similar. This suggests that in the two-photon resonant, multiphoton ionization dissociation of benzene that the initial two-photon absorption step is rate determining in the formation of different ionic fragments at the laser intensities used. This assumption was previously made for the ionization process in MPI polarization studies.<sup>28</sup>

Currently, the vast majority of work involving the multiphoton ionization mass spectra of molecules has been done through the use of high-power lasers that produce nanosecond pulses. Only recently has MPIDMS work appeared that use picosecond pulsed lasers,<sup>57-59</sup> one of which was on benzene.<sup>57</sup>

Observations on the ionization and dissociation of benzene might argue against the superexcited-state mechanism for this system. Divalent benzene cation ( $C_6H_6^{2+}$ ) is not observed in the MPID mass spectra despite the fact that its formation threshold of 26 eV<sup>145</sup> is lower than the appearance potential of the  $C^+$  ion, which is observed. This points to preferential switching within the ionic manifold in favor of smaller daughter ions whenever possible.

Pandolfi et al.<sup>139</sup> have performed experiments designed to examine whether or not neutral fragments ionize and therefore contribute to the overall ion current observed for smaller fragments. This was done through the use of a variable repelling voltage study. In this

two-color experiment, the repelling voltage of a time-of-flight instrument is varied at constant laser powers, wavelengths, pulse widths, and delays between pulses. High repelling voltages have the effect of moving ions created by the first pulse out of the focus of the second pulse. Therefore, only neutral fragments created by the first pulse would be subjected to the second pulse. Comparison of the mass spectrum at high repelling voltages to the mass spectrum taken at low repelling voltages at different wavelengths of the delayed laser could in principal access the presence of and the mass spectrum resulting from the interaction of the second laser pulse with any neutral fragment generated by the first laser pulse. In benzene, neutrals contribute negligibly to the mass spectrum, in agreement with the conclusions of Boesl et al.<sup>60</sup>

Two metastable transitions involving the elimination of H and  $H_2$  to form  $C_6H_5^+$  and  $C_6H_4^+$  from the molecular ion have recently been reported by Boesl et al.<sup>136</sup> In this experiment, a reflectron-type time-of-flight instrument<sup>146</sup> was employed to extend the detectability of metastable peaks to approximately 25  $\mu$ s. A single-color technique was utilized with 259.01-nm radiation. The reported mass resolution of the device was 3900 at 78 amu.

Bernstein and Newton used both electron impact and high-power pulsed lasers to study the fragmentation behavior of benzene and several of its monosubstituted analogues.<sup>147</sup> Concerning benzene, several experiments were performed. In the first of these, electron impact (EI) was used to ionize and fragment benzene in the source of a modified, commercial time-of-flight mass spectrometer. The resulting ensemble of ions was then subjected to the 560-nm, 29 mJ/pulse output of a flashlamp-pumped dye laser. Mass spectra were then recorded as a function of the electron energy. By subtracting the EI mass spectra from the EI/laser modified mass spectra, it was possible to determine which ions were being generated and which were being fragmented by the laser radiation. The overall ion current remained constant, indicating that no new ions were generated by the laser pulse alone. By recording a series of difference spectra at several different electron energies, Bernstein and Newton<sup>147</sup> were able to quantitatively determine the fragmentation routes of each ion in the mass spectrum. It was noted that in comparison to similar experiments done on monosubstituted benzenes, there was no major fragmentation pathway for the benzene radical cation. This was shown to be the case by the large number of small fragment ions that grew in at the expense of relatively incomplete destruction of the parent ion. Ion cyclotron resonance results<sup>148</sup> reveal that at 560 nm, at least two photons are needed to reach the appearance potential of the energetically least expensive daughter fragment.

In another series of experiments,<sup>147</sup> the wavelength dependences of the EI/laser experiments were taken. The results indicated that there was not an appreciable difference in the resulting difference spectra between 413 and 433 nm and 20-eV electron impact.

An inference is made that the benzene ion as well as the smaller fragments can photodissociate over the entire visible spectrum. The energy of two such photons easily exceeds the appearance potential of many daughter fragments from the ground state of the mo-

lecular ion thereby supporting this argument. The lack of wavelength dependence could also be explained in terms of vibrational excitation remaining in the molecular ion after preparation by electron impact. This might tend to wash out any wavelength dependence in the resulting photodissociation spectrum.

Perhaps the strongest support for the mechanism suggesting that the parent ion is the precursor of all the smaller ion fragments in benzene came from the study of the kinetic energy of the electrons ejected in the MPI process.<sup>81,106</sup> The kinetic energies of the ejected electrons fell within a very narrow region suggesting that continuum absorptions leading to the formation of superexcited states and the subsequent ejection of electrons differing in energy by  $h\nu$  may be ruled out. Furthermore, dissociation to smaller species followed by ionization (i.e., the DI mechanism) can also be ruled out for benzene since the different neutral fragments would give electron kinetic energy distributions different from that of benzene. The work of Long et al.<sup>80</sup> reveals the vibrational structure within the multiphoton-induced photoelectron spectrum of benzene. Analysis of such results should provide clues as to the geometry of the ion as well as the nature of intermediate electronic states that were used to ionize the molecule.

Approximately  $3000\text{ cm}^{-1}$  above the  $A \leftarrow X$  transition in benzene, a sharp decrease in the fluorescence quantum yield is observed in conjunction with a rapid increase in absorption line broadening. The exact cause of this observation, which is commonly called "channel three" has been the subject of an active area of research.<sup>149,150</sup> Recently, multiphoton ionization photoelectron spectroscopy (MPIPES) has been used in an attempt to elucidate the dynamical mechanisms giving rise to channel three.<sup>151,152</sup>

Upon excitation to the ground ionic state via a one-photon resonant, two-photon ionization process via the  $S_1$  ( ${}^1B_{2u}$ ) state, benzene undergoes very little geometric change indicating that  $\Delta v = 0$  is the most probable transition.<sup>151</sup> This "selection rule" was utilized to study intramolecular vibrational redistribution (IVR) that is occurring within the  ${}^1B_{2u}$  manifold by monitoring the photoelectron signal as a function of excess energy above the  ${}^1B_{2u}$  origin. Because of the  $\Delta v = 0$  rule, vibrational modes that are populated within the  ${}^1B_{2u}$  state should be populated within the ground state of the molecular ion, assuming that IVR doesn't occur. If however, IVR occurs before the second photon can be absorbed to yield the molecular ion, all memory of the initially prepared state is lost. Instead, ionization occurs from any one of a number of isoenergetic states, which will lead to their corresponding vibrational states of the molecular ion being populated.<sup>151</sup> The photoelectron spectrum of benzene prepared in this manner contains readily identifiable vibrational features as well as a broad, featureless background.<sup>151</sup> Achiba et al.<sup>151</sup> observed that with increasing energy above the  ${}^1B_{2u}$  origin, the broad, featureless portion of the photoelectron signal increased relative to the sharp photoelectron signal. This was attributed to an increase in the IVR rate with increasing excess energy above the  ${}^1B_{2u}$  origin.<sup>151</sup>

Considering the laser power and lens focusing parameters that could be used to estimate the ionization rate, Achiba et al.<sup>151</sup> were able to determine the mag-

nitude of the IVR rate to be around  $10^{10-11}\text{ s}^{-1}$ <sup>151</sup> and hence concluded that IVR was the responsible mechanism for channel three in benzene.

## 2. 2,4-Hexadiyne

By calculating the ionization rate as a function of laser peak power and focusing parameters, Achiba et al.<sup>151</sup> were able to estimate the rate of a dynamical process that was occurring on a time scale 2 orders of magnitude faster than the laser pulse duration. The rates of dynamical processes occurring on the picosecond time scale have been measured by El-Sayed et al. for 2,4-hexadiyne<sup>58,153-155</sup> and more recently for *m*-dichlorobenzene.<sup>156</sup> These experiments use mass analysis instead of photoelectron analysis (although it would be expected that photoelectron analysis might yield complementary information). More importantly however, these sets of experiments utilized a picosecond laser source<sup>58,153-156</sup> vs. the nanosecond source used by Achiba et al.<sup>151,152</sup> to measure the dynamical processes occurring within the neutral and ionic manifolds. Through the use of a two-color pump–pump technique in which the relative delays between the two picosecond laser pulses ranges from picoseconds to nanoseconds, it was shown that it was possible to measure dynamical processes occurring on both the nanosecond and picosecond time scales simply by observing changes in the mass spectra that occur via the multiphoton ionization dissociation process.

In one experiment, the second (532 nm) and fourth (266 nm) lines of a Nd:YAG laser, producing 25-ps pulses, are used. The ionization potential of 2,4-hexadiyne is less than 9 eV meaning that it can be ionized with two 266-nm photons. The 532-nm laser pulse and the 266-nm laser pulse are separated by a variable delay ranging from 0 to 10 ns. Ionization occurs via a one-photon resonant absorption through  $S_1$  followed by the sequential absorption of two 532-nm photons. In the absence of the 266-nm laser pulse, no ion signal is observed, indicating that the 532-nm laser pulse alone is of insufficient intensity to cause ionization. When the 532-nm laser pulse precedes the 266-nm laser pulse, the ion signal produced is identical to that produced from the 266-nm pulse alone. When the 532-nm laser pulse follows the 266-nm laser pulse, the parent ion signal decreases slightly. When, however, the two laser pulses overlap in time, the parent ion signal more than doubles. A plot of the parent ion intensity vs. relative delay yields a spike at zero delay whose width is approximately 50 ps. This feature is virtually identical to a standard autocorrelation trace that was used to determine the pulse width of the laser. This indicates that the process giving rise to the spike at zero delay is significantly shorter than the pulse width of the laser. This result can be explained in terms of a very rapid radiationless process occurring from the  $S_1$  state of the molecule against which the addition of the 532-nm laser pulse helps to compete. This process is faster than the laser pulse meaning that transient absorption of the 532-nm laser photons can only occur when the two laser pulses are overlapped in time.

## 3. Benzaldehyde

Benzaldehyde displays different fragmentation behavior than benzene under similar excitation conditions.

The overall efficiency of ionization is approximately 2 orders of magnitude smaller for benzaldehyde than for benzene even under conditions of one-photon resonant, two-photon ionization through  $S_2$ .<sup>137</sup> At threshold power densities for the observation of ion signal, using 266-nm excitation, the molecular ion is not the dominant species observed.

Benzaldehyde was one of the first molecules studied by MPIDMS. Antonov et al.<sup>63</sup> employed a two-color technique in conjunction with a magnetic mass analyzer to study its ionization and fragmentation behavior. In this experiment, two fixed-frequency lasers were used. The first was a nitrogen laser (3.7 eV), which excited benzaldehyde to its  $S_1$  state. The second pulse was from a hydrogen laser (7.7 eV), which ionized the excited benzaldehyde. By varying the delay between the two fixed-frequency laser pulses, it was possible to probe the up-pumping kinetics of the ionization process. Even with delays in the hundreds of nanoseconds, no significant decrease in the overall ion current was detected even though one photon from each laser was needed to reach the ionization continuum and neither alone had sufficient power to allow a multiple-photon direct ionization to occur. The decrease that was measured was directly attributable to the movement of ions out of the common focus of the two pulses. This indicates that the lifetime of the excited state is very long. Antonov et al.<sup>63</sup> proposed an explanation involving a rapid intersystem crossing into the triplet manifold followed by direct ionization from the triplet state.

The extensive fragmentation that is observed and the low levels of ion signal, even under the favorable ionization conditions of a one-photon resonant (with the  $S_2$  state), two-photon ionization scheme suggest that benzaldehyde may dissociate before it ionizes under certain experimental conditions.

This hypothesis was suggested by Antonov in an attempt to explain observations utilizing 249-nm excitation.<sup>133</sup> Similar results, utilizing 193-nm photons were reported by DeCorpo.<sup>137</sup> Ion signals 2 orders of magnitude lower for benzaldehyde than for benzene were recorded even though 193-nm radiation is resonant with the strong  $S_2$  band of that molecule, and two 193-nm photons would easily exceed its ionization potential of 9.51 eV.<sup>137</sup>

El-Sayed et al.<sup>157</sup> noted that the fragmentation pattern of benzaldehyde displays a strong wavelength dependence. Utilizing 266-nm radiation, as with 249- and 193-nm radiation,<sup>140</sup> it is impossible to exclusively generate the parent ion of that molecule under any condition of laser power. The  $C_6H_5^+$  daughter may be generated as the predominant ion only near threshold. This is not surprising considering that at those wavelengths three photons are required to reach the ionization continuum. Three 266-nm photons leave the molecular ion with approximately 4 eV of excess internal energy ( $3h\nu - IP$ ). Therefore, if the parent ion were formed before the neutral fragmented, it might be endowed with too much excess internal energy to remain intact.

However, if one uses radiation at around 260 nm, it is possible to reach the ionization continuum via a one-photon resonant (via the  $S_2$  state), two-photon ionization process endowing the parent ion with little if any excess internal energy. Under these conditions,

it was still impossible to generate exclusively the parent ion.<sup>157</sup> This suggests that the molecule might be dissociating before it ionizes. Furthermore, comparison of the parent-like species with the  $C_6H_5^+$  daughter fragments as a function of laser power suggests that there is a competition between dissociation into  $C_6H_6$  and CO followed by ionization and fragmentation of  $C_6H_6$  and ionization followed by fragmentation of the parent molecule. The power-dependence results are similar for both the two-photon ionization process (260 nm) and the three-photon process (266 nm).

If the system is excited within the  $S_1$  manifold ( $\pi^* \leftarrow n$ ), it is possible to generate the parent ion exclusively under conditions of moderately low laser power. Utilizing 355-nm radiation which would be one-photon resonant with the  $S_1$  state of benzaldehyde, it should be possible to ionize the system via a one-photon resonant, three-photon ionization process that would endow the molecular ion with about 1 eV of excess internal energy. Careful power-dependence studies comparing the parent ion to the  $C_6H_5^+$  daughters at 355 nm suggest that only one mechanism is responsible for the observed ionization/fragmentation behavior.

These results suggest that the actual fragmentation pattern generated is intimately related to the intermediate states that are used to connect the ground state of the system to the ionization continuum. If one of the intermediate electronic states ( $S_2$  in the case of 266 nm and 260 nm excited benzaldehyde) is dissociative, it may never be possible to observe the parent ion. If however, it is possible to overcome this pathway by increasing the laser power, it may become possible to "protect" the parent ion simply by increasing the laser power. If, on the other hand, the intermediate state does not undergo any type of decomposition ( $S_1$  in the case of 355 nm excited benzaldehyde) it should be possible to observe the parent ion exclusively under threshold-power conditions.<sup>157</sup> The amount of excess internal energy that the molecular ion is endowed with also contributes to the observed fragmentation pattern. In the case of the three-photon ionization utilizing 266-nm radiation, the parent ion will have more than 4 eV of excess energy. On the other hand, in the three-photon ionization of benzaldehyde using 355-nm radiation, the molecular ion will have only about 1 eV of excess internal energy. Therefore for this study, it was necessary to obtain the two-photon ionization mass spectrum with 260-nm laser light. In this manner, a molecular ion with essentially no excess internal energy could be obtained and compared to the three-photon process with 355-nm radiation in which the molecular ion also had very little excess internal energy.

Multiphoton ionization induced photoelectron spectra of benzaldehyde have been reported by Long.<sup>80</sup> Comparisons were made between the MPI photoelectron spectrum generated by benzaldehyde and that generated by benzene using a time-of-flight photoelectron energy analyzer. It was shown that the results are identical when using 258.9-nm radiation. This laser wavelength excites the  $6^1$  transition within the  ${}^1B_{2u}$  manifold of benzene and excites within the  $S_2$  vibronic manifold of benzaldehyde. Two such photons are sufficient to ionize either molecule with little excess internal energy going to the ion. It is suggested that under these experimental conditions, benzaldehyde is

fragmenting via a rearrangement process to form molecular benzene, which in turn ionizes.

#### 4. Acetaldehyde

Because acetaldehyde has a low symmetry ( $C_s$ ), all transitions are both one- and two-photon allowed. One reason that it was chosen for study was to try to understand its apparently large two-photon cross section and the nature of the intermediate states involved.<sup>158</sup>

The MPI spectrum of acetaldehyde has been recorded in a parallel-plate cell in the 358–368-nm region,<sup>158,159</sup> in which the two-photon energy is resonant with the  $3s \leftarrow n$  Rydberg transition. The Rydberg nature of this two-photon resonant state has been confirmed by the observation of a broadening of the spectral features with the addition of  $\sim 80$  atm of argon. The  $55\,040.9\text{ cm}^{-1}$  transition was assigned as  $3s \leftarrow n$ . A detailed vibrational analysis in the region close to the origin shows that most of the activity is due to the torsional vibration ( $V_{15}$ ) and the CCO deformation ( $V_{10}$ ).<sup>158,159</sup> The vibrational analysis also shows that the molecule remains planar in the resonant state and that the methyl group torsional barrier has a value of  $750 \pm 25\text{ cm}^{-1}$  in this excited state, compared to  $413\text{ cm}^{-1}$  in the ground state.<sup>158,159</sup> Theoretical calculations<sup>158,160</sup> as well as experimental results<sup>158,160</sup> establish no change in the methyl-group conformation upon excitation, i.e., one of the methyl-group hydrogens is in-plane and *x-cis* to the oxygen atom, although these calculations fail to reproduce the experimentally observed barrier in the excited state.<sup>158,160</sup> The extraordinarily intense MPI signal from acetaldehyde is likely due to the near resonance of the first absorbed photon with the ( $n, \pi^*$ ) state.<sup>158</sup> The circular-to-linear polarization ratio of ion intensities is found to vary from 0.08 to 0.8 depending upon the laser power and sample pressure. This range of values reflects the additional polarization effects of the postresonant ionization step(s).<sup>158</sup>

The MPI mass spectra of acetaldehyde using ( $0 \leftarrow 0$ ) and ( $v'_{10} \leftarrow 0$ ) two-photon resonant transitions show extensive fragmentation of acetaldehyde under certain experimental conditions.<sup>48</sup> Different ionic species such as  $\text{CH}_2\text{CHO}^+$ ,  $\text{CH}_3\text{CO}^+$ ,  $\text{CHO}^+$ ,  $\text{CH}_4^+$ ,  $\text{CH}_3^+$ , and  $\text{CH}_2^+$  are observed. These individual ion yields have been recorded in the 360–364-nm region, and their variation with laser power has been investigated at both the origin and ( $v'_{10} \leftarrow 0$ ) transitions.<sup>48</sup> Although a considerable deviation from a simple power law can be found for some of the fragments, the dependences go approximately as  $I^p$  where  $p = 1.17 \pm 0.07$  for  $\text{CH}_3\text{CHO}^+$ , up to  $p = 3.54 \pm 0.09$  for  $\text{CH}_3^+$ , for the two-photon resonant transition through the origin.<sup>48</sup> The total ion production (collected in the mass spectrometer) varies as  $I^p$  with  $p = 2.19 \pm 0.08$  for that same transition.<sup>48</sup>

One of the more interesting results in the MPI mass spectra of acetaldehyde is the formation of  $\text{CH}_4^+$ .<sup>48,159</sup> In order to study the rearrangement process that the system must undergo in order to generate this species, MPI and MPI mass spectra of deuterated acetaldehydes were taken.<sup>159,161</sup> The MPI mass spectra of  $\text{CH}_3\text{CDO}$ ,  $\text{CD}_3\text{CHO}$ , and  $\text{CD}_3\text{CDO}$  have been studied in the wavelength region corresponding to the two-photon resonant  $3s \leftarrow n$  Rydberg transitions in a parallel-plate cell.<sup>159</sup> The origins are at  $55\,111.9$ ,  $55\,138.0$ , and  $55\,209.2\text{ cm}^{-1}$ .<sup>159</sup> Vibrational analysis confirms that

the molecule remains planar in the resonant state and that the methyl group torsional barriers have values of  $770 \pm 25$  and  $780 \pm 25\text{ cm}^{-1}$  in the respective molecules compared to the ground state values of  $413$ ,  $410$ , and  $408\text{ cm}^{-1}$ .<sup>159</sup>

MPI mass spectrometry has been carried out on  $\text{CD}_3\text{CHO}$  at the origin of the two-photon resonant  $3s \leftarrow n$  Rydberg transition at  $55\,138.0\text{ cm}^{-1}$ .<sup>161</sup> Variation of individual ion signals is obtained as a function of laser flux.<sup>161</sup> Higher energy threshold fragments are found to exhibit a greater degree of scrambling (with some variation of scrambling with laser flux). In the case of the  $\text{CD}_3^+/\text{CD}_2\text{D}^+$  ion pair, the  $\text{CD}_2\text{H}^+$  scrambled product dominates, although in no case does the scrambling reach the statistical limit obtained by assuming that all hydrogenic species are chemically equivalent. The lower energy fragments  $\text{CD}_3\text{CO}^+/\text{CD}_2\text{HCO}^+$  and  $\text{CHO}^+/\text{CDO}^+$  exhibit behavior that is very far from statistical, while the higher energy fragments are within a factor of 2 of the statistical limits.<sup>161</sup> The isotopic selectivity of the MPI mass spectra for mixtures of  $\text{CD}_3\text{CDO}/\text{CH}_3\text{CHO}$  is demonstrated. The partially deuterated products in these MPI mass spectra are not found, indicating that the scrambling in  $\text{CD}_3\text{CHO}$  is intramolecular rather than collisionally induced.<sup>161</sup>

#### 5. Aniline

Under 266-nm laser excitation of aniline, a broad, asymmetrically distorted mass peak at  $m/e$  66 is observed. This peak has been suggested to result from the decomposition of a metastable parent ion to form  $\text{C}_5\text{H}_6^+$  and  $\text{HCN}$ .<sup>162</sup> Several recent MPI mass spectrometric studies have devoted themselves to the study of this decomposition pathway.<sup>162,163</sup> By varying the excitation frequency of the incident laser, it was possible to endow the molecular ion with varying amounts of internal energy. This excess internal energy affects the rate of unimolecular decomposition of the molecular ion. The rate of decomposition may be measured by studying the shapes of the metastable peak as a function of incident laser wavelength.

Further qualitative results involving the MPI mass spectrum of aniline and several of its derivatives are reported by Rettner et al.,<sup>140</sup> Leutwyler et al.,<sup>164</sup> and Boesl et al.<sup>165</sup> Leutwyler<sup>(1)</sup> used aniline as an example of the isotopic selectivity present in the resonantly enhanced two-photon ionization process. Small shifts in the absorption profiles allow one to preferentially ionize one species.

#### 6. Tertiary Amines

The four amines that will be discussed in this section are (1) trimethylamine, (2) triethylamine, (3) triethylenediamine (DABCO), and (4) quinuclidine (ABCO). Trimethylamine and triethylamine represent open-chain amines, and DABCO and ABCO represent caged amines.

The laser wavelength and power dependences of the MPI fragmentation patterns were studied for all four systems.<sup>166</sup> The wavelength region studied corresponds to three- and four-photon ionizations with two-photon energies in resonance with the  $3p$  and  $3s$  Rydberg states. In the 400–530-nm wavelength region  $\text{N}(\text{CH}_3)_3$  ionizes to yield the parent and fragments only by the loss of

an H atom.  $N(C_2H_5)_3$  ionizes to its parent ion and fragments by the loss of a methyl group. The fragmentation patterns in this wavelength region are found to be independent of the laser intensity over a broad range of powers but strongly dependent upon the laser wavelength. This implies that the parent and daughter ions are essentially nonabsorbing at these laser wavelengths, and therefore, the extent of daughter-ion formation is governed only by the amount of excess energy available from the initial three- or four-photon ionization event. However, at shorter wavelengths such as 355 nm, both molecules do begin to fragment more extensively, and the fragmentation patterns become intensity dependent.

DABCO (diazabicyclooctane) and ABCO (azabicyclooctane) have been the subject of several MPI spectroscopic investigations in which the richly structured spectra of these two compounds have been studied.<sup>167,168</sup> These species possess several features that make study by laser multiphoton ionization attractive. The first is the abundance of richly structured spectral lines corresponding to bound Rydberg states, which makes resonance-enhanced MPI and MPIDMS possible. The second is the relatively low ionization potentials of these, as well as the open-chained amines (all <8 eV), which makes ionization possible with the absorption of several low-energy visible photons.<sup>166</sup>

DABCO and ABCO have been the topic of two recent multiphoton ionization mass spectrometric studies,<sup>168,169</sup> in which the fragmentation patterns were studied as a function of laser power and wavelength. As would be expected, it was determined that the extent of fragmentation of the two caged amines increases with increasing laser power.

Perhaps the most interesting conclusion that may be drawn from the comparison of the open and caged amines has to do with the nature of the intermediate resonant states through which the neutral molecules are excited in order to reach the ionization continuum. It has been noted that the open amines consist of relatively diffuse features owing to the large number of conformers associated with each system (i.e., internal rotation of the alkyl groups with respect to one another). In the caged systems however, no such rotations are possible. Therefore, the resultant spectra are much sharper than their open-chained counterparts. It has been shown that because of this, resonant excitation of the caged amines produces a mass spectrum which is extremely dependent upon the laser power, whereas resonant excitation of the open amine is only slightly power dependent over a wide range of laser powers.<sup>166,169</sup>

### 7. Alkylbenzenes and Halobenzenes

DeCorpo et al.<sup>137</sup> reported an MPI mass spectrum taken by using the output of an ArF laser (193 nm) from toluene and compared the results to the conventional EI mass spectra taken at 10 and 70 eV. It was noted that the total ion current observed in the MPI mass spectrum was slightly larger (about  $\times 1.5$ ) than for benzene and more than 2 orders of magnitude larger than the observed ion current in the MPI mass spectrum of benzaldehyde using 6.42-eV (193 nm) photons.

Squire et al.<sup>142</sup> reported wavelength and power dependence on toluene and drew comparisons and contrasts to its behavior compared to benzene and fluoro-

benzene. In the first set of experiments, the laser was tuned to the  $14_0^1$  two-photon  $L_b$  resonance of benzene, fluorobenzene, and toluene at 504.4 nm, 507.6 nm, and 512.4 nm, respectively. As expected, a near quadratic power dependence is observed in the low-power region when measuring the total ion current, indicating that the initial two-photon resonant excitation is the rate-limiting process leading to ionization and fragmentation.

It was interesting to note in this initial experiment that although the power laws were similar, the total ion yield was significantly higher ( $\times 4$ ) for benzene than for either toluene or fluorobenzene. Goodman and Rava<sup>170</sup> have put forth the argument that the amplitude of the two-photon  $14_0^1$  transition in benzene should be independent of the substituent groups. Squire et al.<sup>142</sup> therefore propose the argument that the disparity in the total ion signal at the same laser power between these three compounds is due to the difference in transition probabilities out of the  $L_b$  state rather than the two-photon excitation into it.

By repeating the same experiments at 500 nm for these three compounds, Squire et al.<sup>142</sup> examined the nonresonant excitation behavior. A quadratic power dependence behavior is also observed for all three compounds, even though no real vibronic states within the  $L_b$  envelope are resonant with 500-nm radiation for any of these compounds. This time however, the total ion yields are reversed. That is, at the same laser power, the total ion yields for fluorobenzene and toluene are significantly larger than for benzene. These differences could be explained in terms of the model proposed by Goodman and Rava.<sup>170</sup> The 500-nm off-resonance signal of toluene in this model is significantly less forbidden than for fluorobenzene.

Recently, Meek et al.<sup>91</sup> have reported the vibrational-state distribution of the toluene radical cation from the kinetic energy analysis of the photoelectrons ejected in the multiphoton ionization process. This work represented a significant improvement in the resolution that could be obtained from a time-of-flight photoelectron spectrometer using a multiphoton ionization source. By resolving the vibrational structure within the ground-state ionic manifold, it became possible to accurately determine the ionization potential of the molecule. This is done by subtracting the energy of the most energetic electron observed in the photoelectron spectrum (which would correspond to the origin of the ground-state electronic manifold of the ion) from twice the laser photon energy (assuming a one-photon resonant, two-photon ionization process). By tuning the laser to the  $S_1 \leftarrow S_0$  origin within the neutral manifold, it was possible to generate significant quantities of the ion without any vibrational quanta in its ground electronic state. In no case were any photoelectrons observed that corresponded to the absorption of photons past the ionization threshold.

Anderson et al.<sup>92</sup> have recorded high-resolution photoelectron spectra of chlorobenzene by pumping various vibrational levels of the intermediate  $^1B_2$  state in a one-photon resonant, two-photon ionization process. Again there was never any suggestion of a continuum-continuum absorption leading to a superexcited state and the ejection of photoelectrons more energetic than a single laser photon. Spectra were recorded in a



time-of-flight photoelectron spectrometer using laser energies ranging from about 266 to 270 nm. Four multiphoton induced photoelectron spectra were recorded at wavelengths of 269.9 nm, 267.78 nm, 267.18 nm, and 266.11 nm corresponding to the 0,0 band,  $\nu_{18b}$ ,  $\nu_{6a}$ , and  $\nu_{6b}$ , respectively, within the  ${}^1B_2$  state of neutral chlorobenzene.

It was found that the resultant photoelectron spectra varied dramatically as a function of the intermediate vibronic state. For example, Anderson et al.<sup>92</sup> observed that if the 0,0 transition within the  ${}^1B_2$  state was excited, the chlorobenzene molecular ion was generated almost exclusively in its vibrational ground state. By pumping  $\nu_{18b}$  within the  ${}^1B_2$  manifold of the neutral molecule, it was found that a distribution of vibrational levels within the ion resulted. The largest group of ions was generated with one quantum of  $\nu_{18b}$  excitation. Finally, when the  $6a_0^1$  band was pumped within the  $S_1$  manifold of the neutral molecule, a vibrational progression in  $\nu_{6a}$  in the ion resulted. These observations proved that by tuning to different vibrational levels of the intermediate electronic state, one could control the nature of the final state vibrational modes. This opened up the possibility of populating nontotally symmetric vibrations in the ionic manifold. This cannot be done in conventional photoelectron spectroscopy.

Takenoshita et al.<sup>171</sup> reported the MPI mass spectra of several xylenes utilizing 193- and 248-nm excitation produced from excimer lasers. Aside from the resemblance in the fragmentation patterns, which would not be unexpected considering the similarity between *o*-xylene and *p*-xylene, one interesting result was noted. Using both 193-nm excitation and 248-nm excitation resulted in a one-photon resonant, two-photon ionization process. Using the 193-nm output of an ArF excimer laser, one would expect a larger total ion yield. This is because 193 nm excites the  $S_2$  ( $\pi^* \leftarrow \pi$ ) of *p*-xylene, which has an absorption cross section more than 2 orders of magnitude larger than for the corresponding  $S_1$  ( $\pi^* \leftarrow \pi$ ) transition, which the 248-nm KrF excimer laser excites. In fact, it is observed that the overall ion signal generated by the 193-nm laser pulse is only half of that generated by the KrF laser pulse. It was suggested by Takenoshita et al.<sup>171</sup> that this is due to a decomposition that produces neutral fragments through a superexcited state of *p*-xylene. El-Sayed et al.<sup>157</sup> used a similar explanation to describe the low ion signal intensities that were observed upon  $S_2$  multiphoton excitation of benzaldehyde. At 248 and 193 nm, which excited the  $S_1$  and  $S_2$  states, respectively, of *p*-xylene, the differences in fragmentation patterns were contrasted and several fragmentation mechanisms were proposed.

MPI mass spectra were obtained from *o*-xylene for comparison purposes. The results indicated that except for slight shifts in intensity for several ions the mass spectra were virtually identical to those of *p*-xylene. Comparisons were also made to the 70-eV EI mass spectra in the case of *p*-xylene.

## 8. Phenol

The MPI mass spectrum of phenol under resonant excitation conditions displays two prominent peaks. These are the parent ion and the daughter resulting from the elimination of CO ( $C_5H_6^+$ ).<sup>17</sup> Studies using the

variable repelling voltage technique<sup>139</sup> suggest that ionization precedes dissociation in phenol.

A two-color experiment utilizing a time-of-flight mass analyzer was performed by El-Sayed et al.<sup>17</sup> The two laser frequencies were fixed in two separate experiments. In the first of these experiments, the molecular ion was generated via a one-photon resonant, two-photon ionization process. Then, a second pulse at 532 nm was cofocused with the ionizing pulse at a variable delay ranging from 0 to 50 ns. With the delay of 50 ns, it was observed that the 532-nm pulse selectively fragmented the  $C_5H_6^+$  daughter while leaving the parent ion virtually intact. When the two laser pulses were made coincident in time, it was found that the parent ion fragmented in addition to the daughter. When the experiments were repeated with 355-nm laser radiation used in place of the 532-nm laser radiation, it was observed that the molecular ion was fragmented whether or not the second pulse was delayed from the ionizing pulse.

These results are explained<sup>17</sup> in the context of the electronic states of the molecular ion. These are available from the photoelectron spectra.<sup>172</sup> The first excited state of the molecular ion lies approximately 2 eV in energy higher than the ground state. Absorption of a 532-nm photon from the first excited state would leave the molecular ion with sufficient energy to fragment. However, absorption of a 532-nm photon from the relaxed excited electronic state might have either a small probability or insufficient energy to fragment the parent ion. Absorption of a 355-nm photon from the relaxed state seems to have sufficient energy and absorption probability to cause fragmentation.

What is interesting about the observed results in the above experiments is that the  $C_5H_6^+$  ion fragments under all experimental conditions. From these results, it must be assumed that the  $C_5H_6^+$  species absorbs strongly at both 532 and 355 nm. At the same time, it is known from the photoelectron data that the molecular ion absorbs at 355 nm but not at 532 nm.

## C. Organometallics and Transition-Metal Complexes

The distinguishing characteristic of the MPI mass spectra of this class of compounds is the appearance of just one major peak, corresponding to the bare metal ion, with a few weak peaks corresponding to partially ligated ions in some cases. This is in sharp contrast to the MPI mass spectra of other classes of compounds where, in general, a wide variety of peaks occur corresponding to all degrees of fragmentation. The pioneering work concerning the MPI mass spectra of this class of compounds was performed by Duncan et al.<sup>50</sup> In it, several transition metal carbonyls including  $Fe(CO)_5$ ,  $Cr(CO)_6$ , and  $Mo(CO)_6$  were excited in the 280-nm region utilizing the output of a Nd:YAG pumped dye laser system. This wavelength corresponds to the charge transfer bands of these compounds. The major observation made was that the bare metal ion was the predominant, if not the only, species observed even near the laser power threshold of ion signal detection. Electron impact mass spectra of this class of compounds reveal a strong signal representing the molecular ion.<sup>(173)</sup>

The charge transfer (CT) bands within such compounds are spectrally diffuse, indicating that the cor-

responding CT states are strongly predissociative. Cooling the complexes by the use of a supersonic expansion failed to resolve the spectra.

In the case of  $\text{Fe}(\text{CO})_5$ , which was excited by using 283.3-nm photons in this study, the ionization potential could be reached theoretically with a one-photon resonant, two-photon ionization. From appearance potential data, production of the  $\text{Fe}^{2+}$  ion requires four such photons. Yet,  $\text{Fe}^+$  is the predominant species observed under all experimental conditions. This suggests that the neutral molecule might dissociate before it can ionize and that ionization may be taking place from a bare metal atom, although this is not the only feasible explanation to account for the observed experimental results. If this were the case however, resonances of the bare metal atom should be detected as the dye laser is scanned assuming that they exist in this region of the spectrum. Duncan et al.<sup>50</sup> observed none however. It was reported that the MPI spectra taken were structureless over all wavelengths recorded. As Leutwyler et al. point out,<sup>174</sup> this apparent contradiction could be a result of experimental conditions rather than a lack of available transitions of the bare metal atom. Duncan et al.<sup>50</sup> reported ionization efficiencies close to 100% even under moderate laser powers. Because of this, no variation in the ion signal could be observed as a function of the incident laser wavelength. The high degree of ionization efficiency probably indicates that all intermediate up-pumping steps leading to ionization are being saturated. This was later shown to be the case by Engelking et al.<sup>175</sup>

Because the bare metal ion is observed in these spectra, the unattached ligand (CO) should be available for ionization and detection. It is understandable that no signal corresponding to the CO cation is observed considering that its ionization potential is around 14 eV.<sup>176</sup>

In another study dealing with  $\text{Cr}(\text{CO})_6$  and  $\text{W}(\text{CO})_6$ , Gerrity et al.<sup>177</sup> used the tool ion current generated in the MPI process to measure the ion-production spectrum between 363 and 585 nm, utilizing loose focusing so as to avoid the saturation problem that Duncan et al.<sup>50</sup> encountered in their work. Gerrity et al.<sup>177</sup> observed a number of sharp lines. Most of them have been assigned to transitions within the bare metal atom leading to ionization. Several of them however cannot be assigned to such transitions, leading to speculation that they arise from vibronic progressions of some molecular species on the basis of their regular spacing. As there was no mass analysis in this study, and hence the possibility of determining whether or not some species other than the bare metal ion contributes to the ion current, only the fact that the resonances were very sharp indicated that it was an atomic resonance and hence the bare metal atom that was being dealt with.

In another investigation on  $\text{Cr}(\text{CO})_6$ ,  $\text{Cr}(\text{CO})_3\text{C}_6\text{H}_6$ , and  $\text{Cr}(\text{C}_6\text{H}_6)_2$  performed by Fisanick et al.<sup>178</sup> several observations were made. First, concerning the observations made by Duncan et al.<sup>50</sup> in the 280-nm region (mass resolved) and in the 363–585-nm region by Gerrity et al.<sup>177</sup> (made on the basis of line widths and peak positions from the total ion current),  $\text{Cr}^+$  was indeed the only species observed in the mass-resolved MPI spectrum of  $\text{Cr}(\text{CO})_6$  in the low-energy region (473.3 nm) of the spectrum. This was not the case for  $\text{Cr}(\text{C}-$

$\text{O})_3\text{C}_6\text{H}_6$  however. Significant amounts of  $\text{Cr}(\text{CO})^+$  as well as the bare metal ion were observed in the time-of-flight mass spectrum utilizing 359.3-nm radiation.

The kinetic-energy spectrum of ejected photoelectrons reveals some interesting information about  $\text{Cr}(\text{CO})_6$ . Several weakly resolved peaks are observed which correspond nicely to energy spacings within the lowest levels of the neutral Cr atom. Another peak appears that can only be explained as coming from a photoelectron ejected from the neutral molecule ( $\text{Cr}(\text{CO})_6$ ).

On the basis of the lack of high-energy photoelectrons (i.e., having at least  $h\nu$  kinetic energy), the contribution of a superexcited-state mechanism can be ruled out. However, considering the above-mentioned results on the photoelectron spectrum, there does appear to be a competition between dissociation and further absorption to the ionization continuum within the dissociation and further absorption to the ionization continuum within the laser pulse width. Why then is  $\text{Cr}^+$  the only species observed under all experimental conditions in the MPI mass spectrum of  $\text{Cr}(\text{CO})_6$ ?

Another intriguing aspect of the results of Fisanick et al.<sup>178</sup> was that no ion current corresponding to benzene or its fragment ions was detected. These species (or their fragments) must be present considering the large signal due to the bare metal ion that is observed.

Fisanick et al.<sup>178</sup> propose no explanation for these observations. There are several possible explanations. First, the metal, having a much lower ionization potential than the ligand, will always end up with the positive charge, leaving only benzene or its neutral fragments. Second, the benzene produced could have so much internal energy that the absorption rate at the laser frequencies is small, and third, the benzene produced never encountered any laser photons due to the short laser pulse width. Leutwyler et al.<sup>174</sup> have measured minute quantities of carbon-containing fragment ions in nickelocene and ferrocene and have come up with conclusions much like those of Duncan et al.<sup>50</sup> and Fisanick et al.<sup>178</sup> That is, production of the bare metal ion is efficient even near the threshold of ion detection. The exact details of the ionization/fragmentation mechanism are expected to depend upon such factors as the ionization potential of the ligands relative to that of the metal, the bond strength, and the laser wavelength, power, and pulse width.

#### D. van der Waals Complexes

van der Waals (vdW) complexes can be formed during supersonic expansion of molecules or atoms with a carrier gas. These species are of the forms  $\text{XR}_n$  (where  $n$  is greater than or equal to 1) and  $\text{X}_n$  (where  $n$  is greater than or equal to 2), where X is the seed molecule and R is the carrier gas. The early studies of vdW complexes in supersonic beams were carried out mainly by laser-induced fluorescence (LIF).<sup>64,179–189</sup> It was determined that variation in the carrier-gas pressure had a profound effect upon the position, intensity, and width of some bands in the LIF spectrum. This is a method of identifying features that are attributed to vdW systems. The fluorescence-excitation technique cannot always give unambiguous assignments on the exact chemical compositions of the vdW complexes. Moreover, vdW species that have small quantum yields

of fluorescence or do not fluoresce altogether cannot be studied by this technique.

For these molecules the laser single or multicolor soft multiphoton ionization method with time-of-flight mass spectrometry (MPIMS) for the ion detection is now used.<sup>190,191</sup> Besides the possibility of solving the problem of inadequate fluorescence quantum yield, this more advanced method of detection also has higher sensitivity than LIF due to the high collection and counting efficiencies of ions formed and the absence of interference from scattered laser light, which often renders the LIF technique difficult.<sup>192</sup> Furthermore, the identity of the species formed is easily determined by the MPIMS technique and requires less instrumentation for detection.

In the following subsections the discussion of these complexes will be confined to those that are produced by a supersonic molecular beam and studied by the laser soft two-photon ionization mass spectrometric techniques.

The diagnostic power of the mass-selected (resonant) multiphoton ionization method would be appreciated even more with the large vdW molecules because of the increased limitation of the LIF technique on the unambiguous characterization of such systems. This increased limitation results from the possible existence of hot-band sequences of the low-frequency intermolecular vibrations in the very large vdW molecules even at the low temperatures attainable in supersonic expansions.<sup>193</sup>

### 1. Metal Clusters

The alkali-metal clusters including Na and K have been investigated in a molecular beam by two-color, two-photon ionization together with a mass spectrometer.<sup>194</sup> By irradiating a molecular beam of Na at an oven pressure of about 200 torr and a nozzle diameter of 0.3 mm with 266-nm laser radiation, mass spectra of Na, Na<sub>2</sub>, Na<sub>3</sub>, Na<sub>4</sub> ... Na<sub>21</sub> were obtained.<sup>194</sup> The A ← X vibronic transition of Na<sub>2</sub> was obtained. Perturbations of certain Na<sub>2</sub> A ← X by the triplet state were detected.<sup>194</sup> The two-photon ionization spectrum of Na<sub>3</sub> was taken with the excitation wavelength ranging from 480 to 690 nm. Several new electronic transitions for Na<sub>3</sub> were found.<sup>194</sup> For K<sub>2</sub>, the B ← X vibronic transitions are observed and perturbations by autoionizing levels are detected.<sup>194</sup>

When the output of a high-power pulsed laser impinges upon a refractory metal target that lies within the throat of a supersonic nozzle, it has been shown that it is possible to create and study isolated clusters of atoms originating from the target via MPIDMS.<sup>195-204</sup> Among the species that have been studied are clusters of refractory metals such as tungsten and molybdenum, which possess exceptionally high boiling points (5933 and 4885 K, respectively). Unlike other studies concerned with the supersonic expansion of metal clusters, which involve high-temperature ovens to generate the metal in the gas phase<sup>204,205</sup> and generally result in a limited amount of internal cooling, laser vaporization cluster studies involve only localized heating of the actual target and generally achieve much lower ultimate rotational and vibrational temperatures.<sup>195-203</sup>

Aside from the academic interest of studying the spectroscopy of these species once they are entrained

within the molecular beam lies enormous practical interest. The studies of metal systems have obvious ramifications in such fields as homogeneous and heterogeneous catalysis and solid-state physics. Among the techniques currently being used to study clusters are multiphoton ionization dissociation mass spectrometry<sup>195-205</sup> and laser-induced fluorescence.<sup>206</sup>

Several studies have been performed on copper vapor that has undergone a supersonic expansion.<sup>197,200,201,205</sup> The studies performed by Smalley et al.<sup>197,200,201</sup> utilized the laser vaporization cluster formation technique, whereas the work of Preuss et al.<sup>205</sup> utilized a high-temperature source to generate the copper vapor. The ultimate vibrational and rotational temperatures of the oven-produced copper clusters were much higher than those of the laser vaporization produced copper clusters.<sup>197,200,201,205</sup> Laser-induced fluorescence was used as the detection technique in the oven-produced copper-cluster study of Preuss et al.<sup>205</sup> Resonant, two-photon ionization with mass analysis was used as the detection technique of Smalley et al.<sup>197,200,201</sup> The use of mass analysis permitted identification of absorption bands arising from dimers and from trimers.<sup>197,200,201</sup> Five new electronic band systems between 2690 and 3200 Å were identified for each of the naturally occurring isotopic combinations of the copper dimer (65-65, 63-65 and 63-63).<sup>200</sup> A band system in the 5225-5430-Å region was assigned to a <sup>2</sup>E'' ← <sup>2</sup>E' transition of the copper trimer (which was assumed to have D<sub>3h</sub> symmetry).

Other copper clusters studied by Smalley et al.<sup>200</sup> ranged in size from the monomer up to a cluster containing 29 atoms. The ionization potential, which could not be exactly determined because of the limited number of fixed-frequency lasers available, was observed to drop from 7.72 eV for the isolated copper atom to less than 5.58 eV for Cu<sub>9</sub> to somewhat above 4.98 eV for Cu<sub>29</sub>.<sup>(200)</sup> The work function for bulk copper is about 4.7 eV.<sup>200</sup> In addition to a decrease in ionization potential with an increase in size of the copper cluster, the ionization potential of the cluster also depended upon whether the cluster was made up of an odd or an even number of atoms.<sup>200</sup> This observation was explained by Smalley et al. to be due to the odd electron in odd-number clusters residing in a nonbonding (and relatively low-energy) orbital vs. a strongly bonding orbital for the highest occupied molecular orbital for even-numbered clusters.

The ground state of the chromium atom consists of half-filled atomic orbitals (4s<sup>1</sup>3d<sup>5</sup>). Because of this, one might expect that the isolated chromium dimer would contain a sextuplet bond and hence a very short bond length. Until the development of the laser vaporization technique for the generation of metal clusters, only a small body of experimental data existed on Cr<sub>2</sub>.<sup>207</sup> In this study Cr<sub>2</sub> was generated from the photolysis of Cr(CO)<sub>6</sub>. Because the transient absorption technique being used was not mass selective, it was thought that the signal could also have been due to other photo-products such as CrO<sub>2</sub> or CrC<sub>2</sub>.

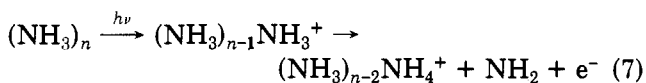
Through the use of the pulsed laser vaporization technique on a chromium target, Smalley et al.<sup>198</sup> were able to determine, through the analysis of the rotational spectrum of Cr<sub>2</sub>, the bond length. A value of 1.68 Å was determined from the rotational constant. This was consistent with the previously determined value from

the flash-photolysis experiments.<sup>207</sup>

In a subsequent set of experiments on the chromium dimer, Riley et al.<sup>199</sup> utilized a similar laser vaporization technique followed by resonant multiphoton ionization mass spectrometry to study the rotational structure occurring within the  $A \leftarrow X$  0,0 band near 459.6 nm. A systematic modulation in the intensity profile of the <sup>52</sup>Cr dimer with localized maxima occurring about every 273 cm<sup>-1</sup> was observed. Closer examination of the rotational peaks near each minimum revealed broadening, which was interpreted as a strong indication that the state was predissociated.<sup>199</sup> The modulation of the rotational envelope was explained in terms of two nearby states, one perturbing and one dissociative.<sup>199</sup>

## 2. Ammonia Clusters

Ammonia clusters and their photochemical products are of special interest because ammonia condenses at pressures and temperatures existing in the atmosphere of Jupiter.<sup>208,209</sup> Ammonia clusters are among the examples whose excited states do not fluoresce. When multiphoton ionization mass spectrometry is applied to the study of weakly bound ammonia clusters, up to the octamer (NH<sub>3</sub>)<sub>6</sub>NH<sub>4</sub><sup>+</sup>, has been found using argon as a seed gas.<sup>210</sup> The initial dilution with argon is expected to promote ammonia cluster formation due to the large cooling effect of the argon in the supersonic expansion. This is evidenced by the increase of NH<sub>4</sub><sup>+</sup>/NH<sub>3</sub><sup>+</sup> ratio with dilution of NH<sub>3</sub> by argon. However, upon further dilution, the ratio goes through a maximum and then decreases, which seems to indicate that supersonic cooling alone is not responsible for the observed change of the ratio. It is also found that the relative intensity of the cluster ion, (NH<sub>3</sub>)<sub>n</sub>NH<sub>4</sub><sup>+</sup>, with respect to the parent, NH<sub>3</sub><sup>+</sup>, is always much stronger under argon-seeded conditions than in pure ammonia, suggesting the cooling effect of argon in the supersonic expansion. Under essentially collisionless conditions, the cluster ions, (NH<sub>3</sub>)<sub>n-2</sub>NH<sub>4</sub><sup>+</sup>, may stem directly from the dissociation ionization of neutral clusters, (NH<sub>3</sub>)<sub>3</sub>, produced in the supersonic nozzle sources



## 3. Benzene vdW Molecules

The ionization potential of benzene-argon complexes has been measured by two-color, resonance-enhanced, two-photon ionization.<sup>191</sup> In these studies, the frequency corresponding to the  $\nu_6$  vibronically excited S<sub>1</sub> state of the complex was chosen as the first laser wavelength. This was found to be red-shifted by about 20 cm<sup>-1</sup> from that of benzene. The second laser wavelength was scanned so that the exact ionization potential of the complex could be determined. The ionization threshold was found to be strongly dependent on the applied electric field, which was required to detect the ionization event.<sup>211</sup> After making the correction for the drawout potential, the ionization potential for the benzene-argon complex is red-shifted by 21.2 meV relative to that of bare benzene. The ionization potential of benzene was found to be 9.24 eV with an onset of 3.2 meV. This shift is due to the electrostatic polarization interactions resulting from the presence of an argon atom in the vicinity of benzene. Since the

binding energy between benzene and argon is fairly small, a large amount of excess energy in any electronic state will result in a high probability of fragmentation. The ability to observe the ionization onset of this complex by the two-color, resonance-enhanced, two-photon ionization technique demonstrates its capability of preparing stable vdW complex ions. The fact that benzene-argon ions are not observed in two-color photoionization when the first excitation wavelength is off-resonance demonstrates the importance of resonant intermediate states in detecting such complex ions.<sup>191</sup>

The benzene homoclusters are formed in a supersonic beam under proper experimental conditions.<sup>190,212,213</sup> The S<sub>1</sub> ← S<sub>0</sub> excitation spectra of the benzene dimer, trimer, and tetramer are obtained by two-color, mass-selective photoionization. All clusters show a weak 0<sub>0</sub><sup>0</sup> band induced by asymmetry in the "crystal field" of the benzene clusters. This induced 0<sub>0</sub><sup>0</sup> band of the clusters is red-shifted from the forbidden monomer origin. The magnitude of this shift increases monotonically with cluster size.<sup>190</sup> The splitting of the 6αbv<sub>1</sub> transition, together with the induced 0<sub>0</sub><sup>0</sup> band, in the dimer indicates an inequality of the two halves of the dimer and favors a T-shaped structure.<sup>190,212,213</sup> From the low-fluorescence quantum yield of the dimer, short lifetime of the dimer 0<sub>0</sub><sup>0</sup> level, and the broadened excitation profile of the dimer 0<sub>0</sub><sup>0</sup> bands, it is suggested that the dimer rearranges from a T-shaped geometry into a sandwich excimer within several picoseconds after laser excitation from the ground T-shaped vdW well.<sup>190</sup>

## 4. The Phenol Dimer and Toluene-Cyanobenzene Complex

The S<sub>1</sub> ← S<sub>0</sub> absorption spectra of the phenol dimer and toluene-cyanobenzene complex in a supersonic free jet have been observed by the use of one-color, one-photon resonant, two-photon ionization in a mass spectrometer.<sup>214</sup> The 0,0 band of the phenol dimer is red-shifted by 303 cm<sup>-1</sup> with respect to that of the phenol monomer. Two low-frequency vibrations at 15 and 112 cm<sup>-1</sup> in the dimer spectrum, which are missing in the monomer spectrum, were assigned as the bending and stretching modes, respectively, of hydrogen bonding. The spectral feature of the toluene-cyanobenzene complex in the 260–280-nm region shows similarity to the spectrum of free cyanobenzene except for a red shift of the band position by 153 cm<sup>-1</sup> and the occurrence of a low-frequency vibration. This indicates that the observed spectrum of the complex may correspond to local excitation of cyanobenzene. The low-frequency progression starts with a spacing of 14 cm<sup>-1</sup> and decreases gradually as the progression proceeds. It ultimately converges into a continuum. This low-frequency progression is attributed to intermolecular vibration.<sup>214</sup>

## 5. Fluorene vdW Molecules

The fluorene-Ar<sub>1</sub>, fluorene-Ar<sub>2</sub>, and fluorene-Kr<sub>1</sub> vdW complexes produced in supersonic expansions were observed and their electronic origins and some low vibrational excitations of the S<sub>1</sub> ← S<sub>0</sub> electronic transition were identified from wavelength-resolved and mass-resolved resonance, two-photon ionization spectra.<sup>193</sup> These electronic origins show red spectral shifts originating from dispersive interactions and possibly also from dipole-induced dipole interactions. The spectral

shifts for fluorene·Ar<sub>1</sub> and for the prominent peak of fluorene·Kr<sub>1</sub> are proportional to the polarizabilities of these rare gases, as expected for both dispersive and for dipole–induced dipole interactions. The spectral shifts for fluorene·Ar<sub>1</sub> and fluorene·Ar<sub>2</sub> are proportional to the coordination number. The vibrationless excitation of both fluorene·Kr<sub>1</sub> and fluorene·Ar<sub>1</sub> near the electronic origins shows a characteristic doublet, the separation of the second weak peak from the main feature being about 40 cm<sup>-1</sup> for the Ar complex and about 30 cm<sup>-1</sup> for the Kr complex. The values favor the excitation of a vibrational mode of the rare-gas atom with respect to the aromatic plane in a single energetically favored structure as the origin of the doublet structure. From the amount of ion current produced at different wavelengths corresponding to different intermolecular fundamentals in the resonant intermediate S<sub>1</sub> state, the lower and upper limits of the dissociation energy, *D*, of the fluorene·Ar<sub>1</sub> complex is the S<sub>1</sub> state can be set as 408 cm<sup>-1</sup> < *D* < 728 cm<sup>-1</sup>.

## 6. Conclusion

It is demonstrated that the laser-resonant, two-color, two-photon soft ionization technique used in conjunction with a mass spectrometer is a powerful tool for the study of complexes formed during supersonic expansions.<sup>190,191</sup> To prepare weakly bound complex ions in their stable states without further fragmentation, proper selection of laser wavelengths and intensities of both colors is required, especially for those vdW complexes involving rare-gas atoms as partners.<sup>212</sup> This is to avoid a large amount of excess energy in any electronic state and thus to decrease the probability of the fragmentation of these complexes. The resonance involved in the intermediate electronic state can also increase the selectivity and sensitivity of the detection. The complexation lowers the ionization potential threshold of the complex by about 50 meV for heterodimers with rare gases<sup>191,212</sup> and by about 500 meV for homodimers.<sup>212</sup> The complexation causes red shifts of the electronic origins relative to those of the monomer X. The amount of red shift seems to be larger for homo-clusters<sup>190,191,212</sup> and increases monotonically with the cluster size X<sub>*n*</sub> (*n* > 2).<sup>190</sup>

## VI. The Future of MPIDMS

In the course of a few years, the field of MPIDMS has developed into a mature branch of research. Its potential use in analytical chemistry is obvious and great efforts in this direction will continue to expand. In the field of physical chemistry, which is the heart of this review, studies that are aimed at an understanding of the dynamics of fragmentation would be most useful. The fact that it is a nonlinear process and the presence of competitive dynamical processes (dissociation, absorption, vibrational redistribution ...) make it very difficult to quantify our interpretations. It makes our results sensitive to laser power, wavelength, pulse width, and the electronic energy levels of the molecule, the parent ions, and the fragment species. Most of this information is lacking. MPIDMS has the same difficulty conventional mass spectrometry studies have. Due to the fact that the ionized electron can carry continuous amounts of kinetic energy, our knowledge of the energy content of a dissociating ion is very un-

certain. In photoionization studies, this problem is eliminated by photoelectron–photoion coincidence techniques. This technique could also be used in MPIDMS.

With all the above mentioned problems, it might be discouraging to continue studies in this field. Scientists never in the past have let difficulties stop them. In fact, the more a field becomes difficult, the more they were challenged. We expect the same will happen in the field of MPIDMS. Below we discuss some of the advantages.

The fact that the absorption process is nonlinear makes the interpretation more difficult, but it also spans the dynamics of the excited states of the molecule and ions. Thus potentially it opens up detailed studies of these processes. This is enhanced by the fact that lasers of picosecond and femtosecond pulse widths can be used. The study of the changes in the mass spectrum produced with two-color picosecond lasers upon changing the delay between the two pulses has recently been shown to give<sup>58,153–156</sup> valuable information in the dynamics of the molecule and its parent ion.

Rapid picosecond and nanosecond dissociation rates can be determined from these techniques. The recent availability of vacuum UV tunable short-pulsed lasers should open up the field of dynamic studies using linear absorption mass spectrometry. Dissociation rates on the microsecond time scale can be determined from the analysis of the line shape of metastable peaks.<sup>162</sup> Longer dissociation rates can be determined through the use of reflectrons.<sup>136</sup>

The use of MPI (to measure the total ion current) in dynamic studies of excited states of molecules is expected to increase. Recently, picosecond pulse width determination was demonstrated with this technique. If the lifetime of the state is slightly longer than the laser pulse width, lifetimes in the picosecond–femtosecond time scale can be determined. Thus, studies combining picosecond lasers with either MPI or MPIDMS are expected to become active. Of course, the need for a continuously tunable picosecond laser is quite obvious.

The analysis of electron kinetic energy will continue in order to obtain information about the ion. Studies of clusters with the use of two-color soft ionization techniques will continue. The fact that soft ionization can keep the clusters intact will make MPIDMS techniques valuable in determining cluster distribution. Such studies would not be as easy using electron impact as it is difficult to endow the molecular ion with a precise amount of internal energy. These, together with many more creative potential future developments, should shape the future of this young field.

*Acknowledgments.* The authors wish to thank the National Science Foundation for their generous support.

## References

- (1) A. Gedanken, M. B. Robin, and N. A. Kuebler, *J. Phys. Chem.*, **86**, 4096 (1982).
- (2) H. M. Rosenstock, Ph.D. Thesis, University of Utah, Salt Lake City, UT (1952).
- (3) H. M. Rosenstock, M. B. Wallenstein, A. L. Wahrhaftig, and H. Eyring, *Proc. Nat. Acad. Sci.*, **38**, 667 (1952).
- (4) H. M. Rosenstock and M. Krauss, *Adv. Mass Spectrom.*, **2**, 251 (1962).
- (5) R. W. Kiser, "Introduction to Mass Spectrometry and its Applications", Prentice-Hall, Englewood Cliffs, NJ, 1965.
- (6) H. M. Rosenstock, *Adv. Mass Spectrom.*, **4**, 523 (1968).



- (7) K. Levsen, "Fundamental Aspects of Organic Mass Spectrometry, Progress in Mass Spectrometry", Vol. 4, H. Budzikiewicz, Ed., Verlag Chemie, Weinheim-New York, 1978.
- (8) W. Forst, "Theory of Unimolecular Reactions", E. M. Loebl, Ed., Academic Press, New York, 1973.
- (9) J. Silberstein and R. D. Levine, *Chem. Phys. Lett.*, **74**, 6 (1980).
- (10) F. Reberstrost, K. L. Kompa, and A. Ben-Shaul, *Chem. Phys. Lett.*, **77**, 394 (1981).
- (11) F. Reberstrost and A. Ben-Shaul, *J. Chem. Phys.*, **74**, 3255 (1981).
- (12) W. Dietz, H. J. Neusser, U. Boesl, E. W. Schlag, and S. H. Lin, *Chem. Phys.*, **66**, 105 (1982).
- (13) J. Silberstein and R. D. Levine, *J. Chem. Phys.*, **75**, 5735 (1981).
- (14) D. A. Lichtin, R. B. Bernstein, and K. R. Newton, *J. Chem. Phys.*, **75**, 5728 (1981).
- (15) D. M. Lubman, *J. Phys. Chem.*, **85**, 3752 (1981).
- (16) N. Ohmichi and R. D. Levine, *Chem. Phys. Lett.*, **90**, 178 (1982).
- (17) R. S. Pandolfi, D. A. Gobeli, J. Lurie, and M. A. El-Sayed, *Laser Chem.*, **3**, 29 (1983).
- (18) J. J. Yang, M. A. El-Sayed, and F. Reberstrost, in preparation.
- (19) C. E. Klots, *J. Chem. Phys.*, **41**, 117 (1964).
- (20) C. E. Klots, *J. Phys. Chem.*, **75**, 1526 (1971).
- (21) C. E. Klots, *Z. Naturforsch. A: Phys. Phys. Chem. Kosmophys.* **27A**, 553 (1972).
- (22) C. E. Klots, *J. Chem. Phys.*, **58**, 5364 (1973).
- (23) C. E. Klots, *Adv. Mass Spectrom.*, **6**, 969 (1973).
- (24) C. E. Klots, *Chem. Phys. Lett.*, **38**, 61 (1976).
- (25) C. E. Klots, *J. Chem. Phys.*, **64**, 4269 (1976).
- (26) M. Quack and J. Troe, *Ber. Bunsen-Ges. Phys. Chem.*, **78**, 240 (1974).
- (27) J. C. Lorquet, *Org. Mass Spectrom.*, **16**, 469 (1981).
- (28) D. H. Parker, J. O. Berg, and M. A. El-Sayed, in "Advances in Laser Chemistry", A. H. Zewail, Ed., Springer Series in Chemical Physics, Vol. 3, Springer-Verlag, Berlin-Heidelberg-New York, 1978.
- (29) K. Levsen, *Adv. Mass Spectrom.*, **8A**, 897 (1979).
- (30) F. M. Devienne and J. C. Roustan, *Org. Mass Spectrom.*, **17**, 173 (1982).
- (31) N. K. Bereshetskaya, G. S. Voronov, G. A. Delone, N. B. Delone, and G. K. Piskova, *Sov. Phys. JETP (Engl. Transl.)*, **31**, 403 (1970).
- (32) S. L. Chin, *Phys. Rev. A*, **4**, 992 (1971).
- (33) R. W. Ditchburn and F. L. Arnot, *Proc. Roy. Soc. London A*, **A123**, 516 (1929).
- (34) A. Terenin and B. Popov, *Phys. Z. Sowjetunion*, **2**, 299 (1932).
- (35) F. P. Lossing and I. Tanaka, *J. Chem. Phys.*, **25**, 1031 (1956).
- (36) H. Hurzeler, M. G. Inghram, and J. D. Morrison, *J. Chem. Phys.*, **27**, 313 (1957).
- (37) H. Hurzeler, M. G. Inghram, and J. D. Morrison, *J. Chem. Phys.*, **28**, 76 (1958).
- (38) N. W. Reid, *Int. J. Mass Spectrom. Ion Phys.*, **6**, 1 (1971).
- (39) P. M. Johnson, M. R. Berman, and D. Zakheim, *J. Chem. Phys.*, **62**, 2500 (1975).
- (40) P. M. Johnson, *J. Chem. Phys.*, **64**, 4143 (1976).
- (41) G. Petty, C. Tai, and F. W. Dalby, *Phys. Rev. Lett.*, **34**, 1207 (1975).
- (42) P. M. Johnson, *Acc. Chem. Res.*, **13**, 20 (1980).
- (43) M. B. Robin, *Appl. Opt.*, **19**, 3941 (1980).
- (44) V. S. Antonov and V. S. Letokhov, *Appl. Phys.*, **24**, 89 (1981).
- (45) R. V. Ambartsumyan and V. S. Letokhov, *Appl. Opt.*, **11**, 354 (1972).
- (46) U. Boesl, H. J. Neusser, and E. W. Schlag, *Z. Naturforsch. A: Phys. Chem. Kosmophys.* **33A**, 1546 (1978).
- (47) L. Zandee, R. B. Bernstein, and D. A. Lichtin, *J. Chem. Phys.*, **69**, 3427 (1978).
- (48) G. J. Fisanick, T. S. Eichelberger IV, B. A. Heath, and M. B. Robin, *J. Chem. Phys.*, **72**, 5571 (1980).
- (49) D. M. Lubman, R. Naaman, and R. N. Zare, *J. Chem. Phys.*, **72**, 3034 (1980).
- (50) M. A. Duncan, T. G. Dietz, and R. E. Smalley, *Chem. Phys.*, **44**, 415 (1979).
- (51) J. H. Glowina, S. J. Riley, S. D. Colson, J. C. Miller, and R. N. Compton, *J. Chem. Phys.*, **77**, 68 (1982).
- (52) P. Agostini, M. Lu Van, and G. Mainfray, *Phys. Lett. A*, **36A**, 21 (1971).
- (53) H. Zacharias, H. Rottke, and K. H. Welge, *Appl. Phys.*, **24**, 23 (1981).
- (54) L. Zandee and R. B. Bernstein, *J. Chem. Phys.*, **71**, 1359 (1979).
- (55) J. P. Reilly and K. L. Kompa, *J. Chem. Phys.* **73**, 5468 (1980).
- (56) S. Rockwood, J. P. Reilly, K. Hohlan, and K. L. Kompa, *Opt. Commun.*, **28**, 175 (1979).
- (57) P. Hering, A. G. M. Maaswinkel, and K. L. Kompa, *Chem. Phys. Lett.*, **83**, 222 (1981).
- (58) D. A. Gobeli, Jack R. Morgan, R. J. St. Pierre, and M. A. El-Sayed, *J. Phys. Chem.*, **88**, 179 (1984).
- (59) A. L. Huillier, G. Mainfray, and P. M. Johnson, *Chem. Phys. Lett.*, **103**, 447 (1984).
- (60) U. Boesl, H. J. Neusser, and E. W. Schlag, *J. Chem. Phys.*, **72**, 4327 (1980).
- (61) J. H. Glowina, R. Romero, and R. K. Sander, *Chem. Phys. Lett.*, **88**, 292 (1980).
- (62) J. B. Hopkins, D. E. Powers, and R. E. Smalley, *J. Phys. Chem.*, **85**, 3731 (1981).
- (63) V. S. Antonov, I. N. Knyazev, V. S. Letokhov, V. M. Matiuk, V. G. Movshev, and V. K. Potapov, *Opt. Lett.*, **3**, 37 (1978).
- (64) R. E. Smalley, L. Wharton, and D. H. Levy, *Acc. Chem. Res.*, **10**, 139 (1977).
- (65) J. B. Hopkins, D. E. Powers, and R. E. Smalley, *J. Chem. Phys.*, **72**, 5039 (1980).
- (66) R. E. Smalley, L. Wharton, and D. H. Levy, *J. Chem. Phys.*, **63**, 4977 (1975).
- (67) T. G. Dietz, M. A. Duncan, M. G. Liverman, and R. E. Smalley, *Chem. Phys.*, **73**, 4816 (1980).
- (68) M. A. Duncan, T. G. Dietz, and R. E. Smalley, *J. Phys. Chem.*, **85**, 7 (1981).
- (69) J. Anderson and J. Fenn, *Phys. Fluids*, **8**, 780 (1965).
- (70) A. Kantrowitz and J. Grey, *Rev. Sci. Instrum.*, **22**, 328 (1951).
- (71) Lasertechnics, Inc., Albuquerque, NM.
- (72) Beam Dynamics, Inc., Minneapolis, MN.
- (73) General Valve Corp., Fairfield, NJ.
- (74) T. E. Adams, B. H. Rockney, R. J. Morrison, and E. R. Grant, *Rev. Sci. Instrum.*, **52**, 1469 (1981).
- (75) D. Bassi, S. Ianotta, and S. Niccolini, *Rev. Sci. Instrum.*, **52**, 8 (1981).
- (76) D. W. Turner, *Adv. Mass Spectrom.*, **4**, 775 (1968).
- (77) Y. Achiba, K. Sato, K. Shobatake, and K. Kimura, *J. Chem. Phys.*, **78**, 5474 (1983).
- (78) Y. Achiba, K. Sato, K. Shobatake, and K. Kimura, *J. Chem. Phys.*, **77**, 2709 (1982).
- (79) J. W. Hepburn, D. Trevor, J. Pollard, D. Shirley, and Y. T. Lee, *J. Chem. Phys.*, **76**, 4287 (1982).
- (80) S. Long, J. Meek, P. Harrington, and J. Reilly, *J. Chem. Phys.*, **78**, 3341 (1983).
- (81) J. Meek, R. Jones, and J. Reilly, *J. Chem. Phys.*, **73**, 3503 (1980).
- (82) J. C. Miller and R. N. Compton, *J. Chem. Phys.*, **75**, 22 (1981).
- (83) J. C. Miller, R. N. Compton, T. Carney, and T. Baer, *J. Chem. Phys.*, **76**, 5468 (1982).
- (84) P. Agostini, F. Fabre, G. Mainfray, G. Petite, and N. Rahman, *Phys. Rev. Lett.*, **42**, 1127 (1979).
- (85) P. Agostini, M. Clement, F. Fabre, and G. Petite, *J. Phys. B*, **14**, L491 (1981).
- (86) R. N. Compton, J. Miller, A. Carter, and P. Kruit, *Chem. Phys. Lett.*, **71**, 87 (1980).
- (87) F. Fabre, P. Agostini, G. Petite, and M. Clement, *J. Phys. B*, **14**, L677 (1981).
- (88) J. Kimman, P. Kruit, and M. van der Wiel, *Chem. Phys. Lett.*, **88**, 576 (1982).
- (89) P. Kruit, J. Kimman, and M. van der Wiel, *J. Phys. B*, **14**, L597 (1981).
- (90) M. White, M. Seaver, W. Chupka, and S. Colson, *Phys. Rev. Lett.*, **49**, 28 (1982).
- (91) J. Meek, S. Long, and J. Reilly, *J. Phys. Chem.*, **86**, 2809 (1982).
- (92) S. Anderson, D. Rider, and R. Zare, *Chem. Phys. Lett.*, **93**, 11 (1982).
- (93) S. Pratt, P. Dehmer, and J. Dehmer, *J. Chem. Phys.*, **78**, 4315 (1983).
- (94) S. Pratt, E. Poliakoff, P. Dehmer, and J. Dehmer, *J. Chem. Phys.*, **78**, 65 (1983).
- (95) P. Kruit, M. van der Wiel, and F. Read In "Laser Techniques for Extreme Ultraviolet Spectroscopy", AIP, New York, 1982.
- (96) M. Lu Van, G. Mainfray, C. Manus, and I. Tugov, *Phys. Rev. Lett.*, **29**, 1134 (1972).
- (97) M. Lu Van, G. Mainfray, C. Manus, and I. Tugov, *Phys. Rev. A*, **7**, 91 (1973).
- (98) A. M. F. Lau, *Phys. Rev. A*, **22**, 614 (1980).
- (99) J. Morellec and D. Normand, *J. Phys. B*, **14**, 3919 (1981).
- (100) D. E. Nitz, P. B. Hogan, L. D. Scheerer, and S. J. Smith, *J. Phys. B*, **12**, L103 (1979).
- (101) C. B. Collins, B. W. Johnson, D. Popescu, G. Musa, M. L. Pascu, and I. Popescu, *Phys. Rev. A*, **8**, 2197 (1973).
- (102) T. P. Martin, *J. Chem. Phys.*, **77**, 3815 (1982).
- (103) K. K. Lehmann, J. Smolarek, and L. Goodman, *J. Chem. Phys.*, **69**, 1569 (1978).
- (104) M. S. De Vries, N. J. A. Van Veen, T. Baller, and A. E. De Vries, *Chem. Phys.*, **56**, 157 (1981).
- (105) F. W. Dalby, G. Petty-Sil, M. H. L. Pryce, and C. Tai, *Can. J. Phys.*, **55**, 1033 (1977).
- (106) J. C. Miller and R. N. Compton, *J. Chem. Phys.*, **75**, 2020 (1981).
- (107) C. Tai and F. W. Dalby, *Can. J. Phys.*, **56**, 183 (1978).

- (108) D. Zakheim and P. Johnson, *J. Chem. Phys.*, **68**, 3644 (1978).
- (109) P. Cremaschi, P. M. Johnson, and J. L. Whitten, *J. Chem. Phys.*, **69**, 4341 (1978).
- (110) H. Zacharias, R. Schmiedl, and K. H. Welge, *Appl. Phys.*, **21**, 127 (1980).
- (111) P. M. Johnson, *Appl. Opt.*, **19**, 3920 (1980).
- (112) G. Radhakrishnan, D. Ng, and R. C. Estler, *Chem. Phys. Lett.*, **84**, 260 (1981).
- (113) E. R. Sirkin and Y. Haas, *Appl. Phys.*, **25**, 253 (1981).
- (114) M. G. White, M. Seaver, W. A. Chupka, and S. D. Colson, *Phys. Rev. Lett.*, **49**, 28 (1982).
- (115) P. Esherick and R. J. M. Anderson, *Chem. Phys. Lett.*, **870**, 621 (1980).
- (116) D. A. Lichtin, L. Zandee, and R. B. Bernstein, In "Lasers and Chemical Analysis", G. M. Hieftje, F. E. Lytle, and J. C. Travis, Eds., Humana, Clifton, NJ, 1981.
- (117) R. V. Hodges, L. C. Lee, and J. T. Moseley, *Int. J. Mass Spectrom. Ion Phys.*, **39**, 133 (1981).
- (118) V. S. Letokhov, *Comments At. Mol. Phys.*, **7**, 107 (1977).
- (119) V. S. Antonov, I. N. Knyazev, V. S. Letokhov, and V. G. Movshev, *Sov. Phys. JETP (Engl. Transl.)*, **46**, 697 (1977).
- (120) B. H. Rockney and E. R. Grant, *Chem. Phys. Lett.*, **79**, 15 (1981).
- (121) R. J. S. Morrison, B. H. Rockney, and E. R. Grant, *J. Chem. Phys.*, **75**, 2643 (1981).
- (122) R. V. Hodges, L. C. Lee, and J. T. Moseley, *Int. J. Mass Spectrom. Ion Phys.*, **39**, 133 (1981).
- (123) G. C. Nieman and S. D. Colson, *J. Chem. Phys.*, **68**, 5656 (1978).
- (124) G. C. Nieman and S. D. Colson, *J. Chem. Phys.*, **71**, 571 (1979).
- (125) J. H. Glownia, S. J. Riley, S. D. Colson, and G. C. Nieman, *J. Chem. Phys.*, **72**, 5998 (1980).
- (126) J. H. Glownia, S. J. Riley, S. D. Colson, and G. C. Nieman, *J. Chem. Phys.*, **73**, 4296 (1980).
- (127) D. H. Parker, R. Pandolfi, P. R. Stannard, and M. A. El-Sayed, *Chem. Phys.*, **45**, 27 (1980).
- (128) A. Gedanken, M. B. Robin, and Y. Yafet, *J. Chem. Phys.*, **76**, 4798 (1982).
- (129) J. Danon, H. Zacharias, H. Rottke, and K. H. Welge, *J. Chem. Phys.*, **76**, 2399 (1982).
- (130) P. M. Johnson, *J. Chem. Phys.*, **64**, 4638 (1976).
- (131) V. Vaida, R. E. Turner, J. L. Casey, and S. D. Colson, *Chem. Phys. Lett.*, **54**, 25 (1978).
- (132) J. O. Berg, D. H. Parker, and M. A. El-Sayed, *J. Chem. Phys.*, **68**, 5661 (1978).
- (133) V. S. Antonov, V. S. Letokhov, and A. N. Shibanov, *Appl. Phys.*, **22**, 293 (1980).
- (134) U. Boesl, H. J. Neusser, and E. W. Schlag, *J. Chem. Phys.*, **72**, 4327 (1980).
- (135) U. Boesl, H. J. Neusser, and E. W. Schlag, *Chem. Phys. Lett.*, **87**, 1 (1982).
- (136) U. Boesl, H. J. Neusser, R. Weinkauff, and E. W. Schlag, *J. Phys. Chem.*, **86**, 4857 (1982).
- (137) J. J. DeCorpo, J. W. Hudgens, M. C. Lin, F. E. Saalfeld, M. E. Seaver, and J. R. Wyatt, *Adv. Mass Spectrom.*, **8A**, 133 (1978).
- (138) M. A. Duncan, T. G. Dietz, and R. E. Smalley, *J. Chem. Phys.*, **75**, 2118 (1981).
- (139) R. S. Pandolfi, D. A. Gobeli, and M. A. El-Sayed, *J. Phys. Chem.*, **85**, 1779 (1981).
- (140) C. T. Rettner and J. H. Brophy, *Chem. Phys.*, **56**, 53 (1981).
- (141) M. Seaver, J. W. Hudgens, and J. J. DeCorpo, *Int. J. Mass Spectrom. Ion Phys.*, **34**, 159 (1980).
- (142) D. W. Squire, M. P. Barbalas, and R. W. Bernstein, *J. Phys. Chem.*, **87**, 1701 (1983).
- (143) L. Zandee and R. B. Bernstein, *J. Chem. Phys.*, **70**, 2574 (1980).
- (144) V. S. Letokhov, *Ann. Rev. Phys. Chem.*, **28**, 133 (1977).
- (145) J. H. Beynon, R. M. Caprioli, W. E. Baitinger, and J. E. Amy, *Org. Mass Spectrom.*, **3**, 963 (1970).
- (146) B. A. Mamyrin, V. I. Karataev, D. V. Shmikk, and V. A. Zagulin, *Sov. Phys. JETP (Engl. Transl.)*, **37**, 45 (1973).
- (147) K. R. Newton and R. B. Bernstein, *J. Phys. Chem.*, **88**, 2246 (1983).
- (148) B. S. Freiser and J. L. Beauchamp, *Chem. Phys. Lett.*, **35**, 35 (1975).
- (149) C. S. Parmenter, *Adv. Chem. Phys.*, **22**, 365 (1972).
- (150) M. Sumitani, D. O'Connor, Y. Takagi, N. Nakashima, K. Kamogawa, Y. Udagawa, and K. Yoshihara, *Chem. Phys. Lett.*, **97**, 508 (1983).
- (151) Y. Achiba, K. Sato, K. Shobatake, and K. Kimura, *J. Chem. Phys.*, **79**, 5213 (1983).
- (152) Y. Achiba, A. Hiraya, and K. Kimura, *J. Chem. Phys.*, **80**, 6047 (1984).
- (153) D. A. Gobeli, J. D. Simon, D. K. Sensharma, and M. A. El-Sayed, *Int. J. Mass Spectrom. Ion Processes*, **63**, 149 (1985).
- (154) D. A. Gobeli, J. D. Simon, and M. A. El-Sayed, *J. Phys. Chem.*, **88**, 3949 (1984).
- (155) M. A. El-Sayed, D. A. Gobeli, and J. Simon In "Ultrafast Phenomena IV", D. H. Austin and K. B. Eisenthal, Eds., Springer-Verlag, New York, 1984, p. 341.
- (156) J. J. Yang, J. D. Simon, and M. A. El-Sayed, *J. Phys. Chem.*, **88**, 6901 (1984).
- (157) J. J. Yang, D. A. Gobeli, R. S. Pandolfi, and M. A. El-Sayed, *J. Phys. Chem.*, **87**, 2255 (1983).
- (158) B. A. Heath, M. B. Robin, N. A. Kuebler, G. J. Fisanick, and T. S. Eichelberger IV, *J. Chem. Phys.*, **72**, 5565 (1980).
- (159) T. S. Eichelberger IV and G. J. Fisanick, *J. Chem. Phys.*, **74**, 5962 (1981).
- (160) R. D. Gordon, *J. Chem. Phys.*, **73**, 5907 (1980).
- (161) G. J. Fisanick and T. S. Eichelberger IV, *J. Chem. Phys.*, **74**, 6692 (1981).
- (162) D. Proch, D. M. Rider, and R. N. Zare, *Chem. Phys. Lett.*, **81**, 430 (1981).
- (163) T. Baer and T. E. Carney, *J. Chem. Phys.*, **76**, 1304 (1982).
- (164) S. Leutwyler and U. Even, *Chem. Phys. Lett.*, **81**, 578 (1981).
- (165) U. Boesl, H. J. Neusser, and E. W. Schlag, *Chem. Phys.*, **55**, 193 (1981).
- (166) D. H. Parker, R. B. Bernstein, and D. A. Lichtin, *J. Chem. Phys.*, **75**, 2577 (1981).
- (167) D. H. Parker and P. Avouris, *Chem. Phys. Lett.*, **53**, 515 (1978).
- (168) D. H. Parker and P. Avouris, *J. Chem. Phys.*, **71**, 1241 (1979).
- (169) D. A. Lichtin, S. Datta-Ghosh, D. R. Newton, and R. B. Bernstein, *Chem. Phys. Lett.*, **75**, 214 (1980).
- (170) L. Goodman and R. P. Rava, *J. Chem. Phys.*, **74**, 4826 (1981).
- (171) Y. Takenoshita, H. Shinohara, M. Umamoto, and N. Nishi, *Chem. Phys. Lett.*, **87**, 566 (1982).
- (172) R. Debies and J. W. Rabalais, *J. Electron Spectrosc. Relat. Phenom.*, **1**, 355 (1972).
- (173) M. R. Litzow and T. R. Spalding, "Mass Spectrometry of Inorganic and Organometallic Compounds", Elsevier Scientific, Amsterdam, 1973.
- (174) S. Leutwyler and U. Even, *Chem. Phys. Lett.*, **84**, 188 (1981).
- (175) P. C. Engelking, *Chem. Phys. Lett.*, **74**, 207 (1980).
- (176) G. Herzberg, "Spectra of Diatomic Molecules", Van Nostrand Reinhold, New York, 1973.
- (177) D. P. Gerrity, L. J. Rothberg, and V. Vaida, *Chem. Phys. Lett.*, **74**, 1 (1980).
- (178) G. J. Fisanick, A. Gedanken, T. S. Eichelberger IV, N. A. Kuebler, and M. B. Robin, *J. Chem. Phys.*, **75**, 5215 (1981).
- (179) R. E. Smalley, L. Wharton, D. H. Levy, and D. W. Chandler, *J. Chem. Phys.*, **68**, 2487 (1978).
- (180) A. Amirav, U. Even, and J. Jortner, *Chem. Phys. Lett.*, **67**, 9 (1979).
- (181) A. Amirav, U. Even, and J. Jortner, *Chem. Phys. Lett.*, **72**, 16 (1980).
- (182) T. R. Hays, W. Henke, H. L. Selzle, and E. W. Schlag, *Z. Naturforsch. A: Phys. Phys. Chem. Kosmophys.*, **35A**, 1429 (1980).
- (183) P. R. R. Langridge-Smith, D. V. Brumbaugh, C. A. Hyanam, and D. H. Levy, *J. Phys. Chem.*, **85**, 3742 (1981).
- (184) A. Amirav, U. Even, and J. Jortner, *J. Phys. Chem.*, **85**, 309 (1981).
- (185) A. Amirav, U. Even, and J. Jortner, *J. Chem. Phys.*, **75**, 2489 (1981).
- (186) T. R. Hays, W. Henke, H. L. Selzle, and E. W. Schlag, *Chem. Phys. Lett.*, **77**, 19 (1981).
- (187) K. H. Fung, H. L. Selzle, and E. W. Schlag, *Z. Naturforsch. A: Phys. Phys. Chem. Kosmophys.*, **36A**, (1981).
- (188) D. E. Powers, J. B. Hopkins, and R. E. Smalley, *J. Phys. Chem.*, **85**, 2711 (1981).
- (189) H. Abe, N. Mikami, and M. Ito, *J. Phys. Chem.*, **86**, 1768 (1982).
- (190) J. B. Hopkins, D. E. Powers, and R. E. Smalley, *J. Phys. Chem.*, **85**, 3739 (1981).
- (191) K. H. Fung, W. E. Henke, T. R. Hays, H. L. Selzle, and E. W. Schlag, *J. Phys. Chem.*, **85**, 3560 (1981).
- (192) D. L. Feldman, R. K. Lengel, and R. N. Zare, *Chem. Phys. Lett.*, **52**, 413 (1977).
- (193) S. Leutwyler, U. Even, and J. Jortner, *Chem. Phys. Lett.*, **86**, 439 (1982).
- (194) A. Herrmann, S. Leutwyler, E. Schumacher, and L. Woste, *Chem. Phys. Lett.*, **52**, 418 (1977).
- (195) T. G. Dietz, M. A. Duncan, D. E. Powers, and R. E. Smalley, *J. Chem. Phys.*, **74**, 6511 (1981).
- (196) D. L. Michalopoulos, M. E. Geusic, S. G. Hansen, D. E. Powers, and R. E. Smalley, *J. Phys. Chem.*, **86**, 3914 (1982).
- (197) D. E. Powers, S. G. Hansen, M. E. Geusic, A. C. Pulu, J. B. Hopkins, T. G. Dietz, M. A. Duncan, P. R. R. Langridge-Smith, and R. E. Smalley, *J. Phys. Chem.*, **86**, 2566 (1982).
- (198) J. B. Hopkins, P. R. R. Langridge-Smith, M. D. Morse, and R. E. Smalley, *J. Chem. Phys.*, **78**, 1627 (1983).
- (199) S. J. Riley, E. K. Parks, L. G. Pobo, and S. Wexler, *J. Chem. Phys.*, **79**, 2577 (1983).
- (200) D. E. Powers, S. G. Hansen, M. E. Geusic, D. L. Michalopoulos, and R. E. Smalley, *J. Chem. Phys.*, **78**, 2866 (1983).

- (201) M. D. Morse, J. B. Hopkins, P. R. R. Langridge-Smith, and R. E. Smalley, *J. Chem. Phys.*, **79**, 5316 (1983).
- (202) D. L. Michalopoulos, M. E. Geusic, P. R. R. Langridge-Smith, and R. E. Smalley, *J. Chem. Phys.*, **80**, 3556 (1984).
- (203) M. E. Geusic, M. D. Morse, and R. E. Smalley, *J. Chem. Phys.*, **82**, 590 (1985).
- (204) S. J. Riley, E. K. Parks, C. R. Mao, L. G. Pobo, and S. Wexler, *J. Phys. Chem.*, **86**, 3911 (1982).
- (205) D. R. Preuss, S. A. Pace, and J. L. Gole, *J. Chem. Phys.*, **71**, 3553 (1979).
- (206) V. E. Bondybey and J. H. English, *J. Chem. Phys.*, **76**, 2165 (1982).
- (207) Y. M. Efremov, A. N. Samoiloova, and L. V. Gurvich, *Chem. Phys. Lett.*, **44**, 108 (1976).
- (208) G. Delacretaz, J. D. Ganiere, R. Monot, and L. Woste, *Appl. Phys. B*, **B29**, 55 (1982).
- (209) T. Owen, *Science*, **167**, 1675 (1970).
- (210) R. Newburn and S. Gulkis, *Space Sci. Rev.*, **13**, 179 (1973).
- (211) H. Shinohara and N. Nishi, *Chem. Phys. Lett.*, **87**, 561 (1982).
- (212) K. H. Fung, H. L. Selzle, and E. W. Schlag, *Z. Naturforsch. A: Phys. Phys. Chem. Kosmophys.*, **36A**, 1257 (1981).
- (213) K. H. Fung, H. L. Selzle, and E. W. Schlag, *J. Phys. Chem.*, **87**, 5113 (1983).
- (214) K. Fuke and K. Kaya, *Chem. Phys. Lett.*, **91**, 311 (1982).